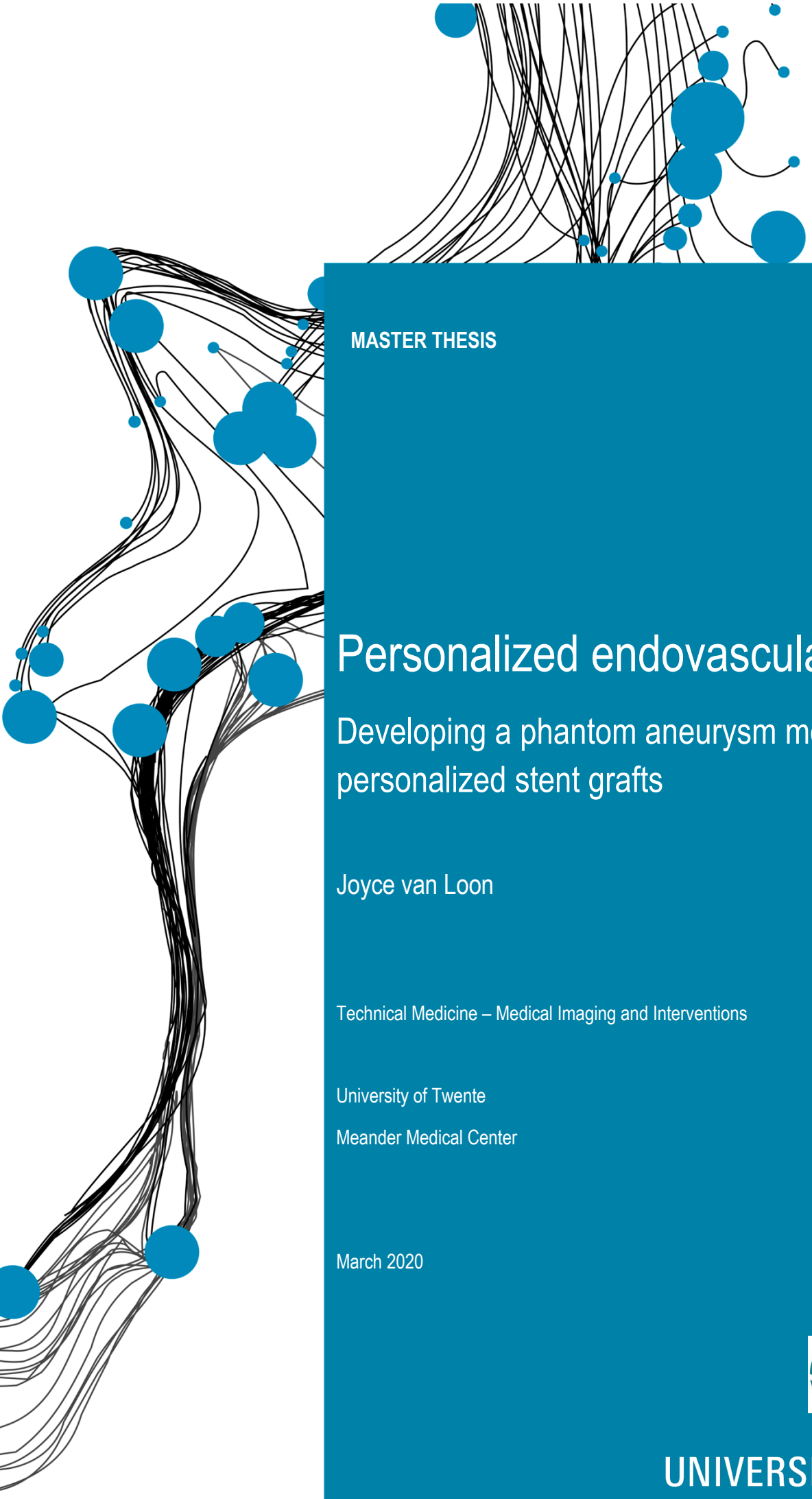

MASTER THESIS

Personalized endovascular stent grafts

Developing a phantom aneurysm model to test personalized stent grafts

Joyce van Loon

Technical Medicine – Medical Imaging and Interventions

University of Twente

Meander Medical Center

March 2020

meander MEDISCH CENTRUM

UNIVERSITY OF TWENTE.

Graduation committee

Chairman	Prof. Dr. Ir. C.H. Slump
Medical supervisor	Dr. V. van Weel
Technical supervisor	Prof. Dr. Ir. C.H. Slump
Process supervisor	R.J. Haarman MSc
Additional supervisor	Prof. Dr. I.A.M.J. Broeders
External member	Dr. E. Groot Jebbink

SUMMARY

This master thesis focusses on the development of personalized endovascular stent grafts and the use of 3D printing. Endovascular stent grafts are used in endovascular aneurysm repair (EVAR). EVAR is a minimally invasive surgery and the gold standard in abdominal aneurysm repair. EVAR excludes the aneurysmal sac, instead of replacing it as in open repair (OR), using a stent graft. This stent graft is often a straight tubular construct. However, the patient's anatomy is often not straight and different morphologies are seen. This might cause an unnecessary high stress on the vessel wall or migration of the stent graft. A higher reintervention rate is seen for EVAR compared with open repair, often due to endoleak or migration of the stent graft. Production of personalized stent grafts might solve these problems, with the result that more patients can be treated endovascular and possible improvement of the clinical outcome.

To compare the straight tubular stent grafts and the personalized stent grafts an aortic model was created. First, a semi-automatic segmentation method was created to obtain the required measurements for the stent grafts. This segmentation was used to create an aorta model and the personalized stent graft. Second, an aortic model and stent grafts were 3D printed. Then the wall distention in the aorta models was measured when a straight stent graft or personalized stent graft were inserted. Metal wires were placed on the 3D printed aorta models and CT-scans were made of the models with the different stent grafts inserted. In the obtained CT-scans the distention of the aortic wall can be measured and the influence of the stents can be evaluated.

The results show that the materials used in this research for 3D printing are sub-optimal. We need a more flexible material for the stent grafts, which has similar properties as the current used nitinol stent grafts. The stent grafts should be foldable to make it possible to place it in the aorta, and ultimately into a delivery system, and expand to a pre-set diameter when placed in the aneurysm. However, in some cases a better sealing with the personalized stent grafts was seen in the obtained CT-scans. The results offer insight in the possibilities and difficulties of 3D printing and the influence of a personalized stent graft in real patient data. Our project shows limitations of our current aortic in vitro model and we provide recommendations for improving our model and experimental setup. Future research should investigate other materials for the aorta models and stent grafts, the properties of these materials and should include various stent designs.

LIST OF ABBREVIATIONS

AAA	abdominal aortic aneurysm
CLL	central lumen line
CT	computed tomography
CTA	computed tomography angiography
EVAR	endovascular aneurysm repair
FEVAR	fenestrated endovascular aneurysm repair
HU	Hounsfield unit
IFU	instructions for use
MRI	magnetic resonance imaging
Nitinol	nickel titanium alloy
OR	open repair
PET	polyethylene terephthalate
(e)PTFE	(expanded) polytetrafluorethylene
SMA	shape memory alloy
SMP	shape memory polymer
STL-file	stereolithography file, standard triangle language, standard tessellation language
US	ultrasound

CONTENTS

INTRODUCTION

ABDOMINAL AORTIC ANEURYSMS

Abdominal aortic aneurysms (AAA) are irreversible localized dilatations of the abdominal aortic vessel, such that the diameter is at least 1.5 times the normal aortic diameter. This abnormal dilatation is caused by a weakness in the vascular wall and involves all three layers of the vascular wall; the intima, the media, and the adventitia. The abdominal aorta begins at the diaphragmatic hiatus and ends in the bifurcation into the iliac arteries. A schematic display of a healthy abdominal aorta can be seen in Figure 1.[1–4]

AAA's are classified by configurations, etiology, and location concerning the origin of the renal arteries. Some of the classifications take the bifurcation of the aorta as well as the involvement of iliac arteries into account. In most cases (up to 90%), the AAA is located distal to the renal arteries. Figure 2 shows a visual representation of this classification by location.[1–3,5]

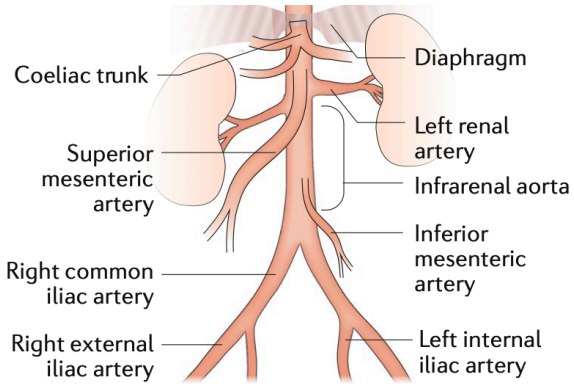

Figure 1: Schematic of a normal abdominal aorta and the major branches.[3]

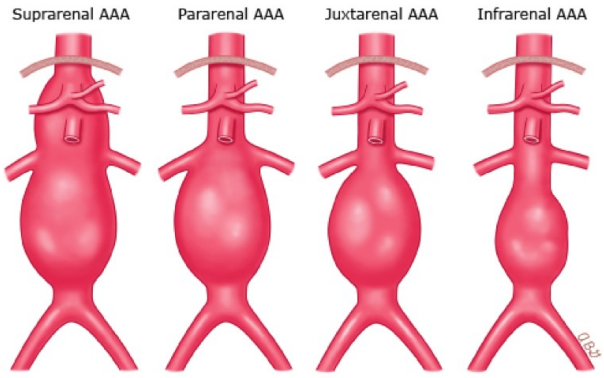

Figure 2: Classification of AAA concerning the renal arteries. Suprarenal AAA includes the origin of renal arteries without the involvement of the superior mesenteric artery. A pararenal or juxtarenal AAA is when an aneurysm originates at the level of the renal arteries. A pararenal aneurysm is when the renal arteries originate from an aneurysmal aorta, and a juxtarenal aneurysm is when the aorta at the level of the renal arteries is normal. An infrarenal AAA originates below the renal arteries with a segment of non-dilated aorta between the renal arteries and the aneurysmal sac. [6]

The prevalence increases with age and aneurysms usually develop after the age of 50 years and are more common in men (1.3% - 8.9%) than in women (1.0% - 2.2%). Other risk factors are smoking, hypertension, chronic obstructive pulmonary disease, coronary artery disease, peripheral arterial disease, obesity, hyperlipidemia, and positive family history. Although prevalence is lower in women, the outcomes are often reported to be worse than those in men, including a higher risk of rupture and more-complicated aneurysm morphology, which makes surgical treatment more difficult.[2,3,7–9]

An aneurysm tends to enlarge over time. Dilatation of the aorta causes increased tension on its wall by the blood that is inside. This continuous enlargement is called the growth of the aneurysm. The mean growth rate is 2.5 mm per year in AAAs of 39 – 49 mm. As the diameter of the aorta increases, the higher the risk of rupture becomes (Table 1).[2,3,7]

Table 1: absolute risk of rupture. [2,7]

Aneurysm diameter	Absolute lifetime risk of rupture
5 cm	20%
6 cm	40%
7 cm	50%

AAA's are multifactorial and often asymptomatic; in some cases lower back and abdominal pain may occur or a palpable pulsatile mass is seen at clinical examination. Diagnosis of an AAA before rupture is essential but is problematic as most AAA stay asymptomatic until rupture. An aneurysm is generally diagnosed incidentally during extensive clinical examination, such as physical examination, ultrasound (US), X-ray (röntgen), magnetic resonance imaging (MRI) or computed tomography (CT). [2,5,7,10,11] Aneurysms with a higher risk of rupture, thus large (asymptomatic) aneurysms or aneurysms that are rapidly growing over a short period are treated by removing the pressure of the aneurysm. It is thought that the benefits of surgery outweigh the risks for an aneurysm diameter of 5.5 cm for men and 5 cm for women. Therefore, the aneurysm diameter is used as a threshold for performing surgery.[1,2,7,10,12,13]

Monitoring the size and growth of the aneurysm is required to prevent rupture. Depending on the aneurysm size (Table 2) this surveillance is needed every six months to three years. However, the condition of the patient is leading when considering surgery. In case the patient is unfit for surgery or with complicated aneurysms, the surgery may be postponed and a larger aneurysm size (>6 cm) is tolerated. Secondly, a much lower threshold of dilatation is warranted for intervention in cases of rapid aneurysm growth (increase in size by 0.5 cm in the last six months) or in patients with certain disorders such as connective tissue disorders, which causes structural changes in the aortic wall. Monitoring the size and growth of the aneurysm is mostly done with US, CT or MRI. [7,8,13,14]

Table 2: Proposed surveillance protocol for patients with AAA.[3]

AAA size (cm)	Men	Women
3.0 – 4.0	Every 2 – 3 years	Every 2 – 3 years
4.0 – 4.5	Every 6 – 12 months	Every 6 – 12 months
4.5 – 5.0	Every 6 months	Every 3 months
5.0 – 5.5	Every 3 – 6 months	Consider surgery
> 5.5	Consider Surgery	

Rupture of an AAA usually leads to sudden onset abdominal or back pain and hypotension or shock. A ruptured AAA is a life-threatening situation with an overall mortality of 90% and even with prompt surgical intervention around 25% of the patients die.[1,2,10,12]

TREATMENT

The goal in the treatment of AAA is to avoid rupture and remove the pressure from the aneurysm, by replacing the aneurysmal sac with a vascular graft. Two surgical treatment options for AAA are open surgery (OR) and endovascular aneurysm repair (EVAR). The decision to offer repair and which type of repair should be performed, is based on several factors, including the size of the AAA, the vascular anatomy, the physical condition (comorbidities of the patient), the quality of life expected post-operatively, risk of aneurysm rupture, and re-intervention rate.[3,15]

Before surgery, preprocedural imaging and planning is critical. CTA (computed tomography angiography) is superior as imaging modality and more accurate than US in estimating the diameters and lengths. During planning the anatomy, the involvement of the visceral arteries, the morphology of the aortic neck (proximal part of the aorta), the aortic angulation, existence of thrombosis, calcifications and stenosis are important factors that should be considered. This indicates the importance of a useful measurement tool in combination with the obtained images to evaluate the condition of the aneurysm and to decide which surgery should be performed and which stent graft is suitable. [16–22]

OPEN REPAIR

Open repair (OR) surgery is performed with laparotomy (Figure 3). An incision from below the sternum to the pubic bone is made to expose the abdominal aorta and aneurysm. Temporarily the blood flow will be interrupted by clamping the aorta on both sides of the aneurysm. Infrarenal clamping is preferred but in juxta- or suprarenal aneurysms, suprarenal clamping may be necessary, and this could lead to an increased rate of renal dysfunction and perioperative morbidity. The aneurysm sac will be cut open and mural thrombus is removed. A (silver-coated) Dacron tube graft is used when the iliac arteries are not involved in the aneurysm. If there are stenosis, occlusions or dilatations in the iliac arteries, a bifurcated graft is used (Figure 4). The graft is sutured into place, just above and below the site of the aneurysm. The clamps will be removed, the graft will be checked for leaks and the aneurysmal sac will be sutured over the graft to protect the graft from exposure to intestines.[3,14,16,21,22]

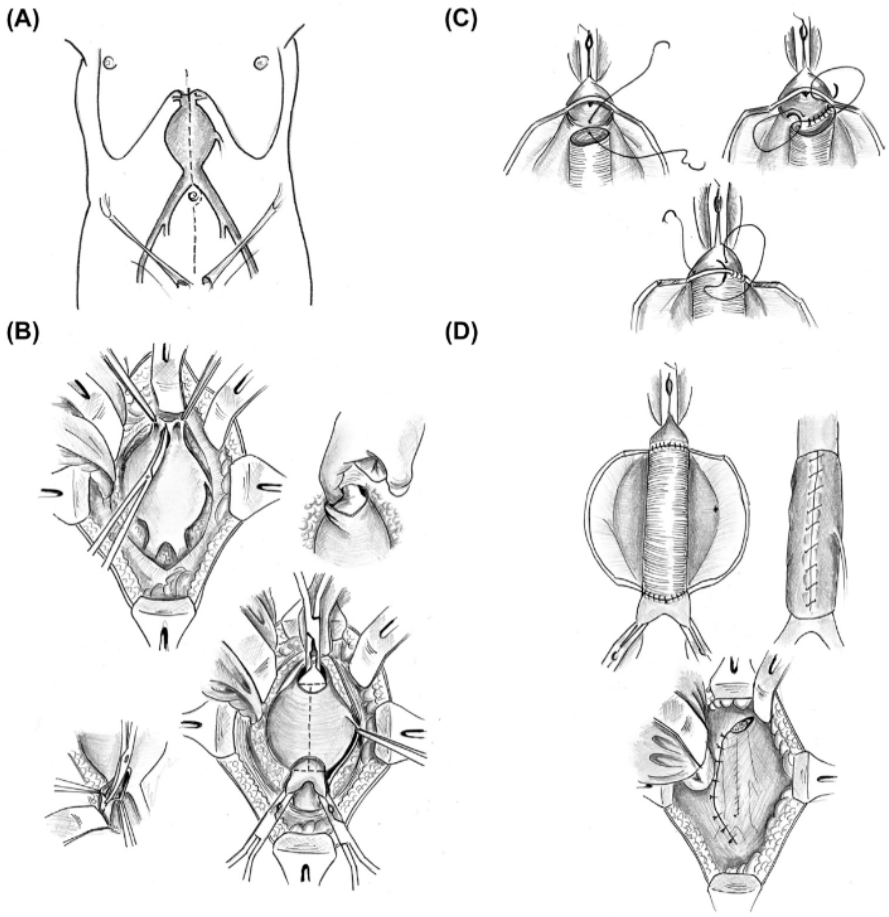

Figure 3: Open repair AAA. (A) midline incision. (B) Dissection of the aneurysm and clamping of the aorta and iliac arteries. The aneurysm sac will be cut open and mural thrombus is removed. (C) Sewing the graft in the aorta, starting posterior. (D) Graft placement. Check for leaks and suturing of the aneurysmal sac over the graft.[21]

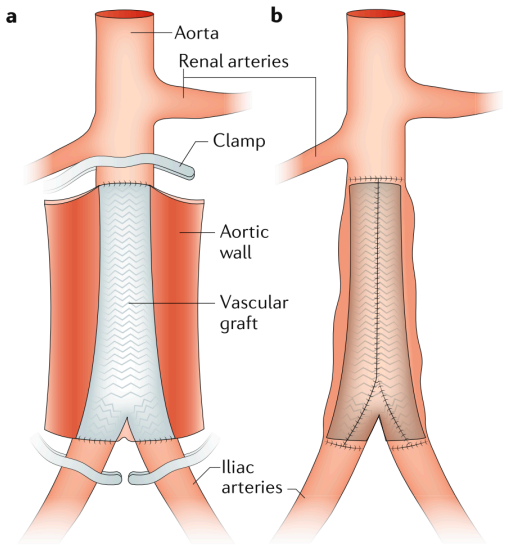

Figure 4: Bifurcated graft, a graft from the aorta to the iliac arteries, is used when the aneurysm involves one or both iliac arteries.[3]

ENDOVASCULAR ANEURYSM REPAIR

EVAR is a minimally invasive procedure. Access to the femoral arteries is obtained through small incisions in both groins or percutaneously (Figure 5). A bifurcated stent graft is inserted via the femoral and iliac arteries and is sutured in the aorta under X-ray guidance, with the use of guidewires, catheters, and a specially designed introducer system. The stent graft is anchored at the normal, non-aneurysmal aorta at the level of the renal arteries (Figure 6). The stent graft acts as a bypass for blood flow through the aneurysm and like this, the aneurysm is excluded from the systemic circulation instead of replaced as in OR.[3,15,16,22]

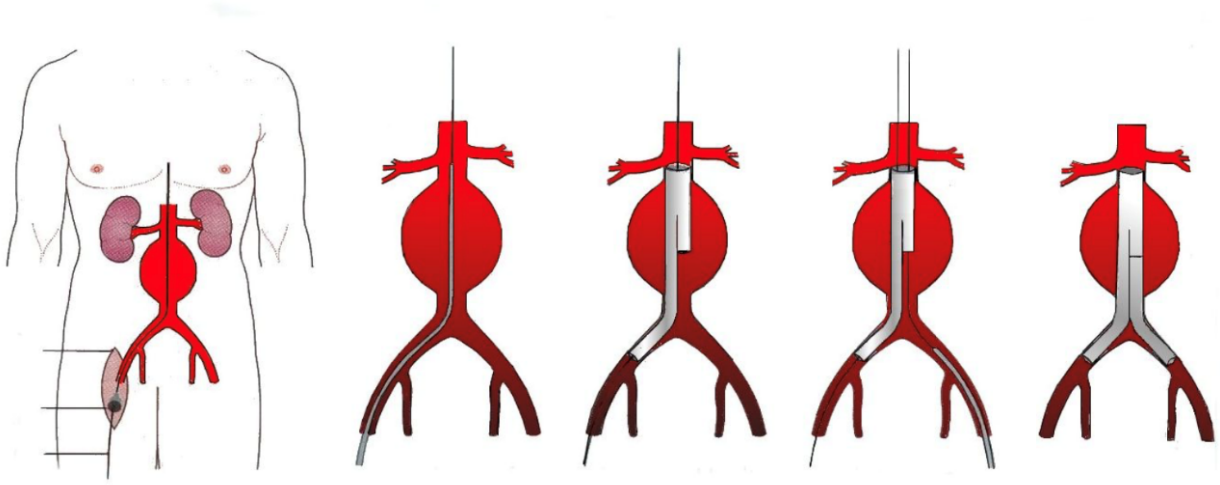

Figure 5: EVAR procedure. The introduction and positioning of the modular stent graft. The stent graft consists of a main device and extensions. The two femoral arteries are the access sites and incisions are made as shown.[16]

The stent grafts consist of a main device and extensions. The stent graft consists of the main body with two legs (one long, one short), a contralateral limb and possible additional stent grafts, including aortic and iliac extensions. First, the main device is positioned, deployed and sealed in the aortic neck. The other parts of the stent are introduced and placed in the main body of the stent graft and the iliac arteries. A control image is made to check the position of the stent graft and prevent over-stenting. At the end control images are made to check for endoleaks (consistent blood flow into the aneurysmal sac). After all the checks, the incision will be sutured.[3,15,16]

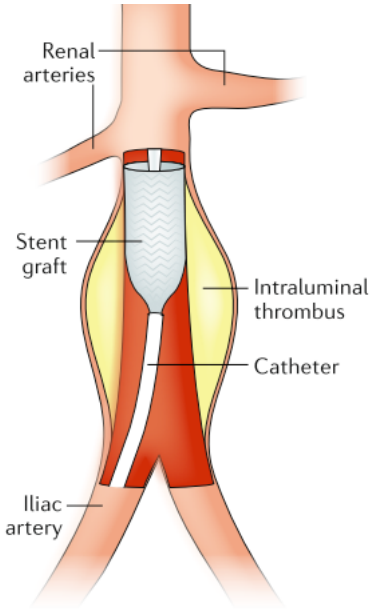

Figure 6: Schematic representation EVAR. A catheter is inserted through the iliac artery, the stent graft is opened and the main upper body is placed (and sealed) below the renal arteries. [3]

COMPARING OR AND EVAR

Several studies have compared OR surgery with EVAR. OR is mainly used for suprarenal AAA or anatomical challenging aneurysms. EVAR is considered minimally invasive and has proven benefits compared with OR; 1% 30-day mortality risk with EVAR compared to the 5% with OR, shorter hospital stay, and faster recovery. However, these studies show no difference in long term overall mortality.[7,16,22,23]

There have been improvements in technology and materials and the long-term outcomes of EVAR with the current methods may improve compared to previous studies. Nowadays, EVAR is preferred in most centers and is a safe alternative to OR. However, when EVAR is not a suitable treatment option or in case of complications after EVAR and in relatively young patients who are fit for surgery, OR is still performed.[17,23–25]

Some patients are not eligible for EVAR, most of them because of a complicated morphology, for example short or inadequate sealing zones or no suitable access vessels. The quality of the access vessels is essential for the introduction of the stent graft. Therefore, the access vessels should be of adequate quality. To anchor the stent graft, a healthy non-aneurysmal part of the aorta below the renal arteries, the sealing zone, is required for complete sealing. The sealing zone should be at least 10-15 mm for a proper and complete sealing. When EVAR is not a suitable treatment option, due to inadequate anatomical suitability, OR or complex EVAR, e.q. FEVAR (fenestrated EVAR) to obtain more proximal seal, should be considered. [3,8,16]

COMPLICATIONS OR AND EVAR

There are several complications of surgical and endovascular treatment of AAA. In OR the most prevalent complications are incisional hernia and sexual dysfunction. Additionally, graft limb occlusion and graft infection are common. In the case of suprarenal clamping, acute renal failure and chronic kidney disease can occur. Graft limb occlusion and stent graft infection can occur after EVAR but is not common. The reintervention rate is higher in EVAR than open repair (26% vs. 12%). Endoleaks are a

frequent indication for reintervention and are the most common complications after EVAR. Endoleak is described as a persistent blood flow outside the endograft and within the aneurysmal sac, which may lead to aneurysm expansion with the risk of AAA rupture. Endoleaks can be classified into five types (Figure 7, Table 3). Endoleak can occur due to incomplete sealing or migration of the stent graft and have an incidence of 14% up to 50%. [16,18,19,22,26–28]

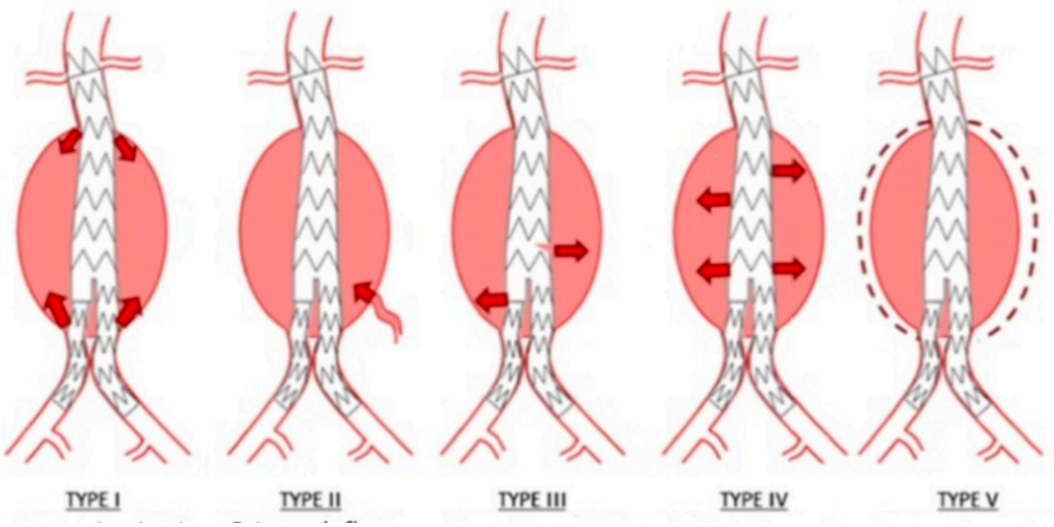

Figure 7: Classification system endoleak. Type I occur due to inadequate sealing and is more common in patients with complex arterial anatomy. Type II is a collateral-vessel leak and is the most common type of endoleak after EVAR and considered benign. Type III is a leak through a defect in the graft. Type I and III are risk factors for rupture. Type IV is caused due to graft-wall porosity and usually resolve spontaneously during the post-procedure period. In type V aneurysm growth is seen but without identifiable endoleaks (type I – IV). [19]

Table 3: Classification of endoleak, the source of blood flow determines the type of endoleak.[16,18,19]

Type I	Inadequate seal at graft ends
A	Proximal graft attachment site leaks
B	Distal graft attachment site leaks
C	Iliac occlude
Type II	**Collateral-vessel leak. Retrograde blood flow through branch vessels, filling the aneurysm sac.**
A	One vessel
B	Two or more vessels
Type III	**Graft failure, leak through a defect in the graft.**
A	Junctional separation of the modular components
B	Fractures or holes involving the endograft.
Type IV	**Graft-wall porosity.**
Type V	**Endotension. Increase in aneurysm diameter, with no identifiable endoleaks.**

Complications are often due to complex arterial anatomy and migration of the stent graft. Examples of complex aneurysm anatomy are short infrarenal necks, angulated necks, tapered necks, or extension of the aneurysm at the level of the renal and visceral arteries.

The standard EVAR procedure is not suitable for up to 30% of the patients with an AAA. For these patients, personalized endovascular stent grafts can be made to fit the patient-specific anatomy. New devices have been developed, such as fenestrated (FEVAR) and branched stent grafts and new techniques have been used where stent graft combinations are created. These techniques extend the graft seal zone to above or at the level of the renal arteries, including stenting of renal arteries or mesenteric arteries. In this way, EVAR can be tailored to fit any patient that requires intervention. In addition, it is reported that aortic neck dilatation for infra-renal stent grafts is 25% and for supra-renal stent grafts 2%. Aortic neck dilatation increases the risk of migration and endoleak and therefore, fenestrated or branched stents may be beneficial to all AAA patients. However, the production of these personalized stent grafts is expensive and has a considerable production time of 6-8 weeks. Therefore, acute treatment with personalized stent grafts is not yet feasible.[16,20,21,29–31]

CASUS

In April 2011 a CT-scan is made from a patient who is occasionally feeling unwell and dizzy, accompanied with hypertension. On the CT-scan incidentally an AAA is seen. In the first three years after diagnosis a stationary aneurysm growth is seen on the US and CT-scans. In the fifth year after diagnosis (in 2016), an aneurysm growth of 9 mm is seen in one year and the aneurysm had a diameter of 4.8 cm. The year after (in 2017) a growth of 5 mm is seen in 9 months. After eight years (in 2019) the aneurysm has a maximal diameter of 6 cm and the patient is discussed for EVAR due to the aneurysm size and rapid growth.

The patient, a male of 81 years old, is known with hypertension, chronic renal insufficiency and foramen stenosis and no other comorbidities are known. The proximal aortic neck is long enough but highly angulated (>90°) which can be seen in Figure 8. No significant calcifications or thrombi were seen. According to the instructions for use (IFU) of Medtronic this patient is not eligible for EVAR. [32] Nevertheless, the patient is treated and an Endurant stent graft is placed successfully (Figure 9). After 8 weeks US images were made and there was no indication for endoleak.

The Medtronic Endurant stent graft is commonly used for EVAR procedures in Meander Medical Center Amersfoort. According to the IFU of Medtronic, the Endurant stent graft can be used in the treatment of infrarenal aneurysms when the aortic neck diameter, defined as the length over which the aortic diameter remains within 10% of the infrarenal diameter, is in the range of 19-32 mm and has no significant calcifications or thrombi (<25% of vessel circumference of aortic neck and iliac artery and <50% of the length of the iliac artery). The landing zone of the stent graft, thus the proximal aortic neck, should be at least 10 mm long. For a proximal neck of ≥ 10 mm and <15 mm, the angle should be lower than 60° and for a neck length of ≥ 15 mm, a maximum angle of 75° is tolerated. This is the angle between the proximal aortic neck and the aneurysmal sac. The last requirement is that the diameter of the chosen stent graft is 10-20% bigger than the measured vessel diameter (i.e. oversizing of 10-20%). [32]

Elements that may affect the outcome are [30,32,33]

- Severe proximal neck angulation (with a short proximal aortic neck)
- Thrombi or calcifications at the arterial implantation sites, specifically the proximal aortic neck and distal iliac artery
- Irregular calcification or plaque may compromise the fixation and sealing of the implantation sites

This patient has a straight but highly angulated (>90°) aortic neck. The AAA has a diameter of 65 mm and the largest diameter of the aortic neck was 27.6 mm. An Endurant stent graft with a diameter of 32 mm is used in this case. As can be seen in Figure 9 the stent graft is highly bended in the aneurysm and this could create unnecessary pressure on the aortic wall and problems with placing the stent graft. A personalized fit would be a solution to reduce the pressure on the aortic wall and create a better fit in the highly angulated aortic neck and increase the operability.

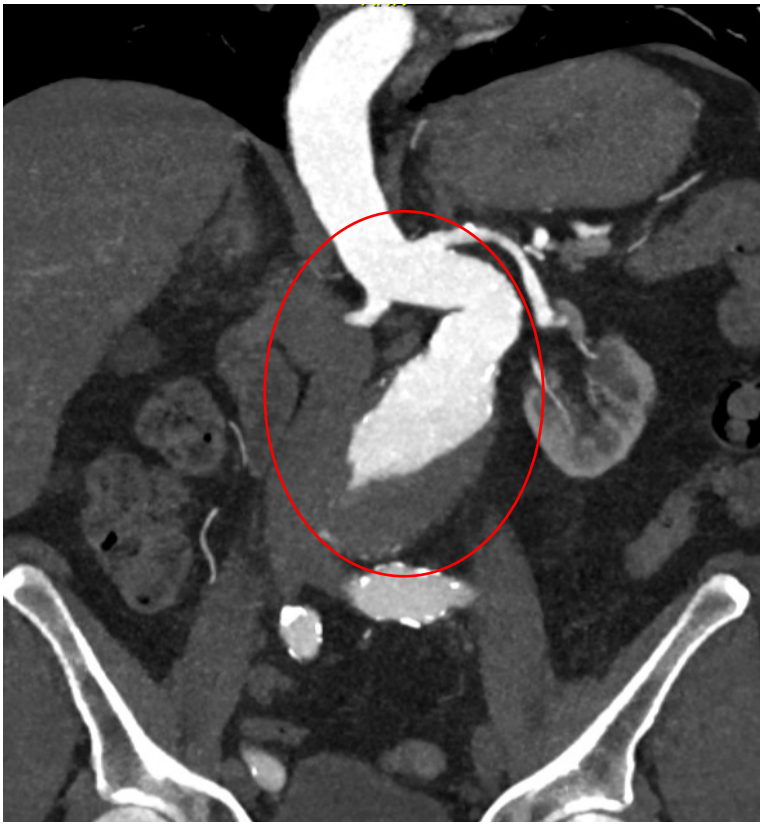

Figure 8: CT-scan of the patient in this casus. A coronal slice of the CT-scan and in the red circle the AAA and a highly angulated aortic neck.

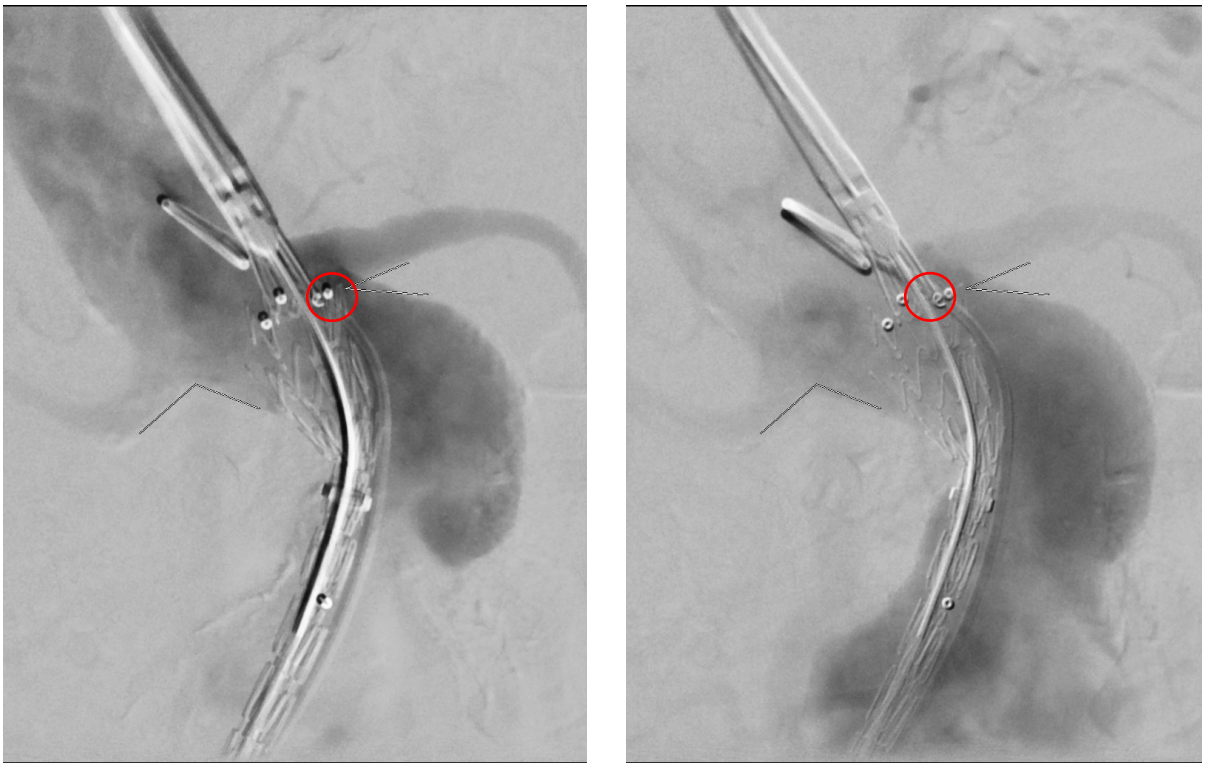

Figure 9: The stent graft positioning and blood flow in the aortic neck and aneurysm. The stent graft is visible with the opaque dots (markers) and the letter e (see red circle), which indicates rotational positioning of the stent graft. The black lines are indicators for the renal arteries.

Research objective

EVAR procedures are preferred over OR, however the high reintervention rates and complications like migration, endoleaks or sac expansion are problematic. With new techniques it is possible to customize the standard stent graft and add fenestrations or branches and create the possibility to treat even complex aneurysms. However, this customizing is a time-consuming and costly process. A faster process to produce personalized stent grafts is required for acute (complex) endovascular treatment of AAA.

Secondly, the stent grafts are often straight tubular constructions and the morphology of the aorta and aneurysm differs from patient to patient. The aortic neck is mostly not straight and is more often tapered, conical, angulated or bulged. Oversizing the stent graft, with 10-20% of the largest measured aortic neck diameter, is considered to compensate for the change in diameter of the aorta and establish an outward pressure of the stent graft on the aortic wall to create a good sealing. However, the oversizing may result in unnecessary high stresses on the vascular wall on the smaller diameters in for example conical or tapered aortic necks. For some patients a straight off-the-shelf stent graft, and therefore EVAR, is not a suitable option due to these anatomical variations.

When we can create personalized stent grafts, with a better fit to the patient's anatomy, more patients can be treated endovascular. We want to study the possibilities of 3D printing endovascular stent grafts and investigate what the differences are between standard off-the-shelf stent grafts and personalized stent grafts. We hypothesize that personalized stent grafts have a better fit to the patient's anatomy (with a smaller oversizing), which results in less pressure on the aorta wall and fewer complications, such as endoleaks, occur. Furthermore, when 3D printing is possible, it is a quicker process to produce personalized stent grafts and even patients in an acute setting (with or without complex anatomy) can be treated.

Previous work on the personalized stent graft from Tim Boers at Meander Medical Center was done in a computer model. The results showed a more equal distribution of the stress and strain in the personalized stent and might thereby induce less stress and strain on the vascular wall. In this study, we will focus on the 3D printing of infrarenal personalized stent grafts (Figure 10). We will first create a (semi-) automatic segmentation method to obtain detailed information about the patient aneurysm morphology. This information is required for the personalization of the stent graft. The personalized stent graft creates an artificial aortic neck for an off-the-shelf stent graft to land on (Figure 10).

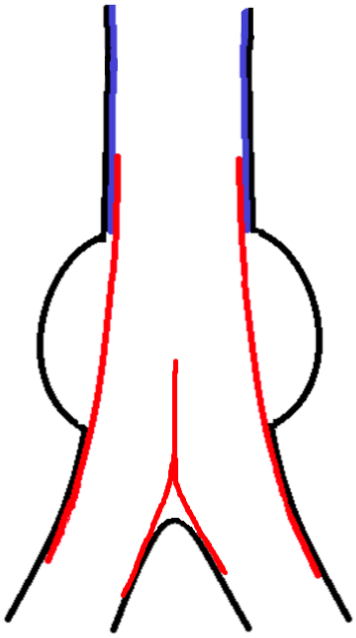

Figure 10: Sketch of the combined custom-made stent graft. The arterial wall shown in black, the personalized stent graft in blue and off-the-shelf stent graft in red. [34,35]

Aim

The overall aim of this research is to improve the (personalized) stent graft for patients with an AAA, both normal and morphologically complex aneurysms. It is thought that 3D printing could be a helpful tool by creating personalized stent grafts and therefore we will explore the possibilities of 3D printing endovascular stent grafts in this study. We hypothesize that personalized stent grafts provide a better sealing with less stress on the aortic wall.

ANALYSIS

STENT GRAFT MATERIAL

The stent graft is manufactured using different materials and made such a way to mimic the mechanical and biological behavior of the artery. The mechanical behavior of an artery is based on the three layers of the wall, the intima, the media, and the adventitia and is mostly dependent on the thickness of the media layer. The media layer of the wall is the thickest layer and consists of elastin, smooth muscle cells, and collagen fibers.
The ideal vascular stent graft is biocompatible, non-thrombogenic, flexible yet robust, and easy to manufacture. To manufacture a stent graft with these capabilities, different materials are used. The endovascular stent grafts consist of multiple parts and different materials.[36,37]

The metal framework or skeleton of the stent is most often made from the self-expandable memory metal nitinol (nickel-titanium alloy). The graft, most often made of a polymer (PTFE; polytetrafluorethylene) or a polyester (PET; polyethylene terephthalate), is fixated to the metal framework to exclude the aneurysm from the blood circulation.

NITINOL

Nitinol is a nickel-titanium shape memory alloy (SMA), composed of approximately 50% nickel and 50% titanium (in biomedical applications 55% nickel is most common). It is known as a thermo-responsive smart material. Smart materials possess the ability to change properties to specific external stimuli and are self-sensing, have self-adaptability, have shape memory, or multiple of these functionalities combined. Nitinol is often used because of its durability, biocompatibility, corrosion resistance and shape memory, which gives the stent the ability to self-expand in the vessel to a pre-set diameter.

The shape memory effect of nitinol consists of two forms: thermal memory and mechanical memory and is possible due to phase transformation (Figure 11). Thermal memory gives nitinol the ability to revert to its initial shape (austenite phase) upon heating after been deformed in the low-temperature phase (martensite phase). Nitinol stents are manufactured above the transformation temperature (austenite phase) and then compressed in a delivery system at a low temperature (martensite phase). In the human body, at the treatment site, the stent is released from the delivery system and expands to the pre-known shape (thermal shape memory effect). [25,37–40] The mechanical memory is also described as super-elasticity and is a reversible response (deformation) to applied stress. When the stresses are removed, the deformation vanishes, and the material recovers to its original shape. This quality is responsible for mimicking the elasticity of the healthy native artery.[36–38,41,42]

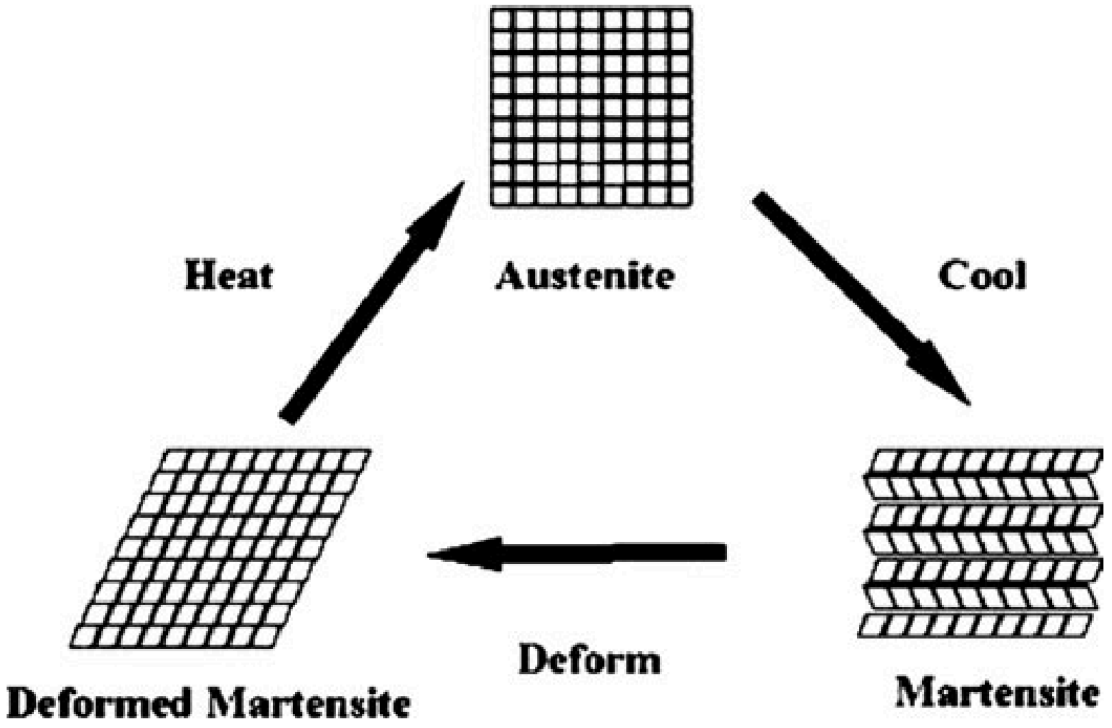

Figure 11: Phase transformation, change of the crystalline structure of nitinol. The martensite and austenite transform into one another. These phase changes can be produced either by thermal or mechanical actions. [40]

GRAFT MATERIAL

Currently, PET and (e)PTFE are the two most used graft materials, due to their biocompatibility, durability and strong wear and tear resistance. PET is a thermoplastic polyester and a durable graft material. PET is used due to its low costs, good performance, and processability. PET is also known by the brand name Dacron, which are synthetic fibers of PET. PTFE is a versatile synthetic polymer and is a biocompatible and highly non-reactive material. PTFE is also known by the brand name Teflon.[36,37,39]

MATERIAL PROPERTIES

Several material properties can be compared, and we will look at the Young's modulus (E), yield stress (σ_Y), tensile strength (σ_{UTS}), and strain (ε). The material properties of nitinol and nitinol-55, the most used composition of nitinol, can be found in Table 4. Stress is the force per unit area and the yield stress is the largest stress that the material can withstand while remaining elastic. If the material is deformed beyond the yield point, the material is not able to return to its original shape when the stress is removed and eventually, it will reach the tensile strength and breaking point. The Young's Modulus and strain reflect the flexibility and stiffness of a material. Strain is the amount of deformation per unit of stress and when stress and strain are plotted (see Figure 12) the Young's modulus can be calculated. The Young's modulus is the slope of the stress-strain curve and represents the force per cross-sectional area which is required to stretch the material to twice its initial length. [4,43]

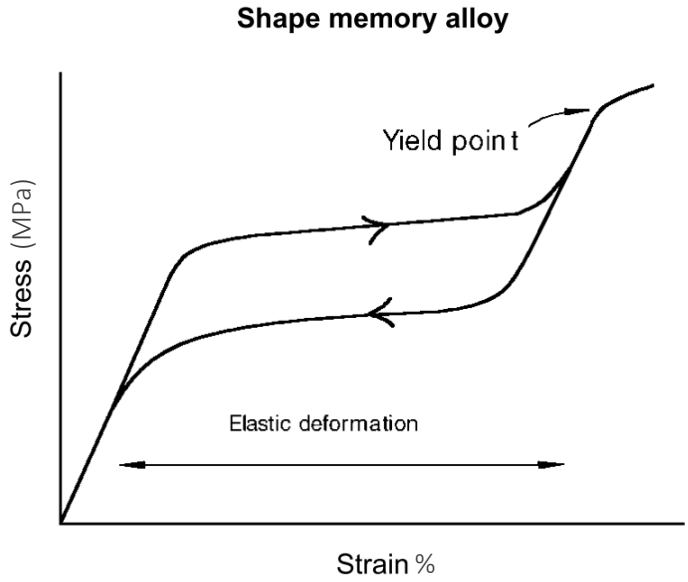

Figure 12: Stress-Strain curve of a shape memory alloy like nitinol. The material is unable to return to its original shape when too much deformation is applied and eventually it will reach its breaking point. [43]

Table 4: Material properties of nitinol and the nitinol-55, which is the most used composition nitinol for medical devices, and the properties of nitinol in combination with the most used graft material (in Meander MC).

	Nitinol [39]	Nitinol-55 [43]	Nitinol & PET [39]
Youngs modulus (GPa)	40	70	-
Yield strength (MPa)	390	103-138	4.6
Tensile strength (MPa)	425	860	59.3
Mean strain (%)	0.04	-	0.06
Strain at break	Strain limit 12%	-	-

METHODS

PATIENTS

PHASE 1

We have performed a retrospective analysis of all AAA patients undergoing (F)EVAR and open repair in 2017-2018 at Meander Medical Center Amersfoort. First, the CT-scans from the patients on the list of aorta aneurysm procedures in 2017 and 2018 (made by the vascular surgeons) in Meander Medical Center Amersfoort were collected.

Inclusion criteria:

- On the abdominal aneurysm procedures list (2017 or 2018) and with available CT-scans.

Exclusion criteria:

- Not in the abdominal aneurysm procedures list
- No CT-scans available

PHASE 2

Information about the anatomical aneurysm location, aortic neck morphology, type of surgery (EVAR, FEVAR or OR), used stent graft and the occurrence of endoleaks and which type of endoleak were obtained from the included patients of phase 1.
Using this information, the patients were in- and excluded regarding the following criteria.

Table 5: Inclusion and exclusion criteria phase 2 of patient selection.

Inclusion	Exclusion
Infrarenal AAA	Juxtarenal AAA
	Suprarenal AAA
	Pararenal AAA
	Other aneurysms (iliac)
EVAR	OR
	FEVAR
Information available about used stent grafts (size and brand)	Incomplete operative report
First intervention	Reintervention
Complete information; check endoleaks (US, CTA-scans)	Incomplete information

PHASE 3

The CT-scans from the included patients of phase 2 were used to segment the aorta aneurysm and these segmentations were used to create 3D models as described in the sections below. From these 3D models a selection, with different aortic neck morphologies, is made for 3D printing. To perform the first tests and to evaluate the materials, the printing method and measurement method we make a selection of patients with different aorta and aneurysm morphology (straight, conical and tapered) for 3D printing the aorta, personalized stent graft and straight stent graft.

PREOPERATIVE IMAGING

Angiographic CT data is obtained by the radiology department. A contrast agent is injected into the bloodstream, which makes visualization of the vascular system on CT-images possible. CT-scans are made from all patients with AAA to measure the dimensions of the aorta and the aneurysm and to determine if surgery is needed and determine the properties of the stent graft. The CT-scans are loaded in 3Mensio (Pie Medical Imaging, The Netherlands), where the dimensions of the aortic neck, aneurysm and the iliac arteries are measured. Based on these measurements is decided what stent graft should be used.

SEGMENTATION

A semi-automatic segmentation method is created to obtain the properties and measurements of the aneurysm from the CT-scans and to create a 3D model.

The requirements of this method and model are:

- A good segmentation of the complete aneurysm
- Diameter and length of the aneurysm can be calculated
- Good segmentation of the aortic neck (for sealing), comparable with the used techniques (3Mensio)
- The segmentation can be used to create a personalized stent graft
- The segmentation can be used to create a 3D model of the aorta
- The created models are 3D printable, a solid and smooth model is therefore required
- Segmentation process takes < 15 minutes and less than 10 user inputs
- Location of the iliac arteries and renal arteries (and other essential arteries when included in the aneurysm)
- Aortic neck angulation can be calculated
- Calcification or stenosis are included in the segmentation, but distinguishable from the blood flow and aortic wall
- Comparable results as the measurements in 3Mensio

A segmentation method was developed in MATLAB (version 2018a, MathWorks Inc.) to semi-automatically segment the aorta from the CT-scans. A thresholding method, using the scan-specific minimal and maximal Hounsfield Unit (HU) from the selected region of interest (ROI), was used for segmentation. All collections of connected voxels are considered and the collection containing the aorta, mostly the largest one, is selected to create a 3D model. This surface model was exported as an STL-file. The created STL-files are imported into Meshmixer (version 2018, Autodesk, Inc.) in which the unnecessary structures from the segmentation can be removed which remains the aortic neck, the aneurysm and the upper part of the bifurcation. The 3D model is inspected on holes and the wall

thickness is set to 2 mm. Then the model is smoothed and scaled. The scaling is performed with the found voxel size and slice thickness in MATLAB from the CT-scans. This model was saved as an aorta model.

The personalized solid stent graft models (without strut-structure) are made from the created aorta models. The suprarenal part of the aorta, the renal arteries, and most of the aneurysm was removed and the remaining aortic neck and the approximately upper 2 cm of the aneurysm are scaled up by 10% in each direction to create the personalized stent graft model (with 10% oversizing).

The standard stent graft models were created in 3ds Max (version 2020, Autodesk Inc.) from a tube with a length of 5 cm and the diameters of the stent graft used for EVAR procedures.

PRINTING

For printing the aorta and stent graft, materials need to be chosen. We will look into the properties of the aorta and nitinol stent grafts and the available materials in the printing labs at the University of Twente.

AORTA

The aortic wall is elastic and has high compliance (Young's Modulus of 0.41 MPa), which is essential for the blood flow. The aorta distends and acts as a reservoir during systole (contraction of the heart) and during diastole (rest phase, heart refills with blood), when the blood pressure falls, the aortic wall returns to its initial state and pushes the blood forward. This is called the Windkessel effect and causes that the aortic pressure does not fall to zero during diastole. [4,44]

For the 3D model of the aorta, we have the following requirements:

- Flexible material; high elasticity
- High compliance (mean artery compliance is 7.4 mm Hg x 10^{-2})
- Comparable Young's modulus to the aortic wall (0.41 MPa) [4,44,45]
- The wall thickness of the abdominal aorta is approximately 1.5mm, therefore a wall thickness of 1, 1.5 and 2 mm should be considered for the 3D models of the aorta. [4,44]
- Durable material; can handle the pressure of the stent graft and for further research the (simulated) blood pressure (mean pressure in the aorta is 95 mm Hg [4])
- Printable in complex shapes
- 3D prints are formable and do not rupture when the stent graft is placed in the model
- Non-permeable for fluids (when used in phantom)

STENT

The stent graft should not have a negative influence on the Windkessel effect in the aorta.

The stent graft material should have a high compliance and needs to mimic the native artery. Nitinol stents have proven to have high compliance due to its super-elasticity, it is biocompatible, hemodynamically stable, fatigue resistant, and non-corrosive.[25,37]

However, we were not able yet to 3D print nitinol and we needed a comparable material to study the behavior of the stent grafts.

The requirements of the stent graft material:

- Flexible and strong material. The stent is foldable and flexible.
- Self-expanding properties, required for placing the stent in the aorta model
- “Soft” material, preventing aorta damage
- Printable in complex shapes

Requirements of the personalized stent graft:

- Customization (and size ranging) possibilities
- Forms to aorta
- Create a good sealing between the aortic wall and stent graft
- Create a good and safe landing zone for the off-the-shelf stent graft

STRAIGHT VERSUS PERSONALIZED

Wall stress is difficult to measure in our model, however, distention of the aortic wall as a result of outward force can be measured. To do so the printed aortas needed to be marked. A measurement tool and method should be created. The marked aortas are scanned with an Iluma Cone Beam CT-scanner (Imtec Imaging, Ardmore OK, USA). First, only the aortas are scanned and then the stented aortas. The X-ray tube was an IAE X20P (imd Generators, Grassobbio, Italy). The detector size is 24.5 cm x 19 cm. The used settings:

- 3.8 mA current
- 120 kV voltage
- 20 seconds scan time

By measuring the distance between the markers in the different CT-scans (only aorta, straight stent and personalized stent), the difference in wall distention can be determined.
Secondly, the seal between aorta and stent graft is reviewed in the made CT-scans.

Requirements of this experiment:

- The stent causes sufficient radial force on the aortic wall (oversizing 10%)
- The used markers are easily to distinguish from the aortic wall
- A clear difference between aorta and stent graft
- Possible to measure the distention of the aortic wall
- Seal zone visible
- Sealing can be evaluated
- Measurements can be done with the CT-scans, with the use of MATLAB

RESULTS

PATIENTS

PHASE 1

On the list of AAA repairs of 2017 and 2018, 53 patients and 48 patients are present, respectively. This results in 101 patients who are treated with an EVAR procedure between 01-01-2017 and 31-12-2018. From these 101 patients we were not able to obtain the CT-scans for 23 patients of the list of 2017 and 13 patients of the list of 2018, which results in a total of 65 patients whom we obtained the pre-operative CT-scans and are included in this phase of patient selection.

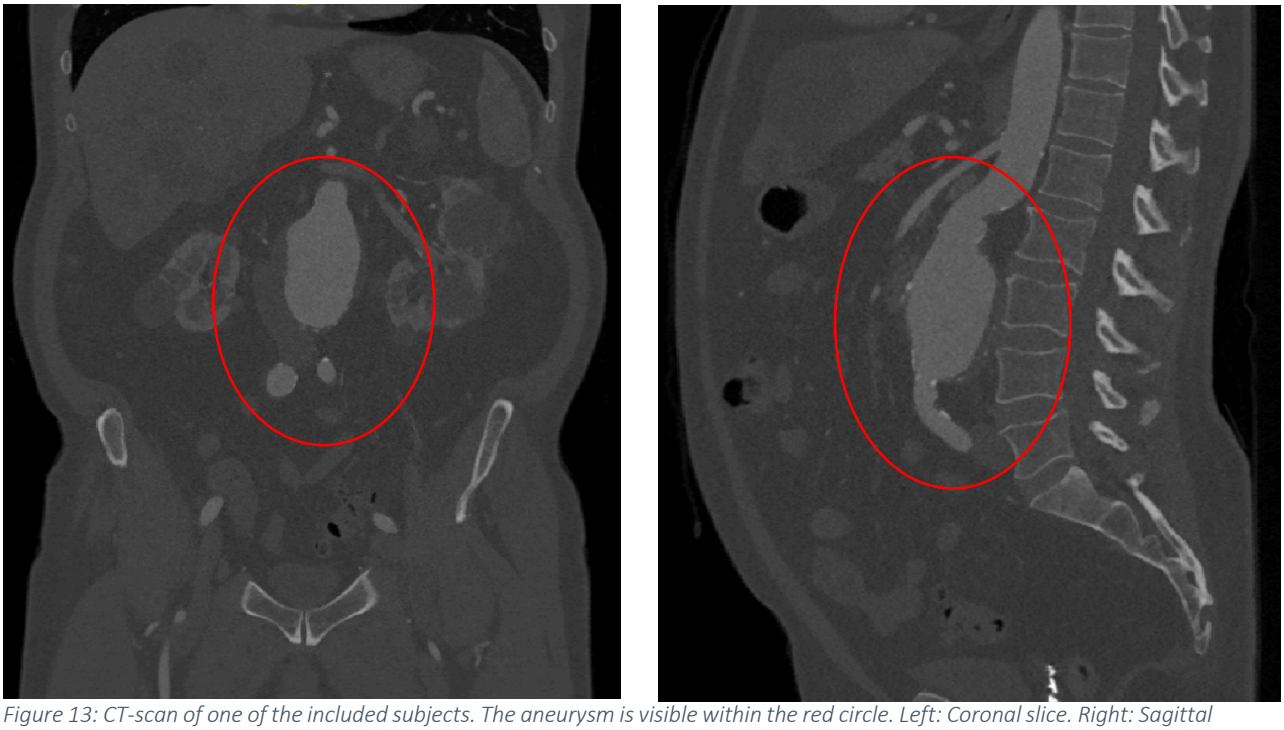

Figure 13: CT-scan of one of the included subjects. The aneurysm is visible within the red circle. Left: Coronal slice. Right: Sagittal slice.

PHASE 2

Information about the anatomical location of the aneurysm, aortic neck morphology, type of surgery (EVAR or FEVAR), used stent grafts and the occurrence of endoleaks and which type of endoleak were obtained from the included patients of phase 1. 58 patients were included for the next phase, regarding the in- and exclusion criteria.

Table 6: Excluded patients regarding the exclusion criteria.

Exclusion	Reason
2 patients	Incomplete operative report
1 patient	Not an AAA, other aneurysm
1 patient	Extension stent graft (aneurysm above the placed stent graft)
3 patients	FEVAR

PHASE 3

From the 58 included patients of phase 2, we were able to segment the aorta and the aneurysm from the CT-scans of 43 patients (Figure 13). From the CT-scans of 15 patients we could not segment the aorta and aneurysm properly, due to a small difference in HU of the aneurysm and surrounding structures.

Figure 14: Segmentation abdominal aorta aneurysm of one of the included subjects. Left: the MATLAB segmentation results. Right: the Meshmixer results, where a large part of the renal arteries, the mesenteric artery and the iliac arteries are removed.

SEGMENTATION

We were able to segment the aneurysms of 43 patients (example is shown in Figure 14). These segmentations were imported to Meshmixer and 3D models were created (Figure 14 and 15). We could not create a 3D model for 4 segmentations, due to too many irregularities in and around the aneurysm and aorta. This results in 39 3D models of the aorta and aneurysm, which are used to create stent graft models. For these 39 patients, we searched for the used stent grafts implemented during EVAR and

create a personalized stent graft. We selected 5 patients (Table 7) with different aorta and aneurysm morphology for 3D printing the aorta, personalized stent graft and straight stent graft. All these patients are male, between 61 and 74 years old and only subject 1 had an endoleak type Ib and subject 3 and 5 had an endoleak type II. For the endoleak type Ib, in subject 1, a reintervention is performed after one year.

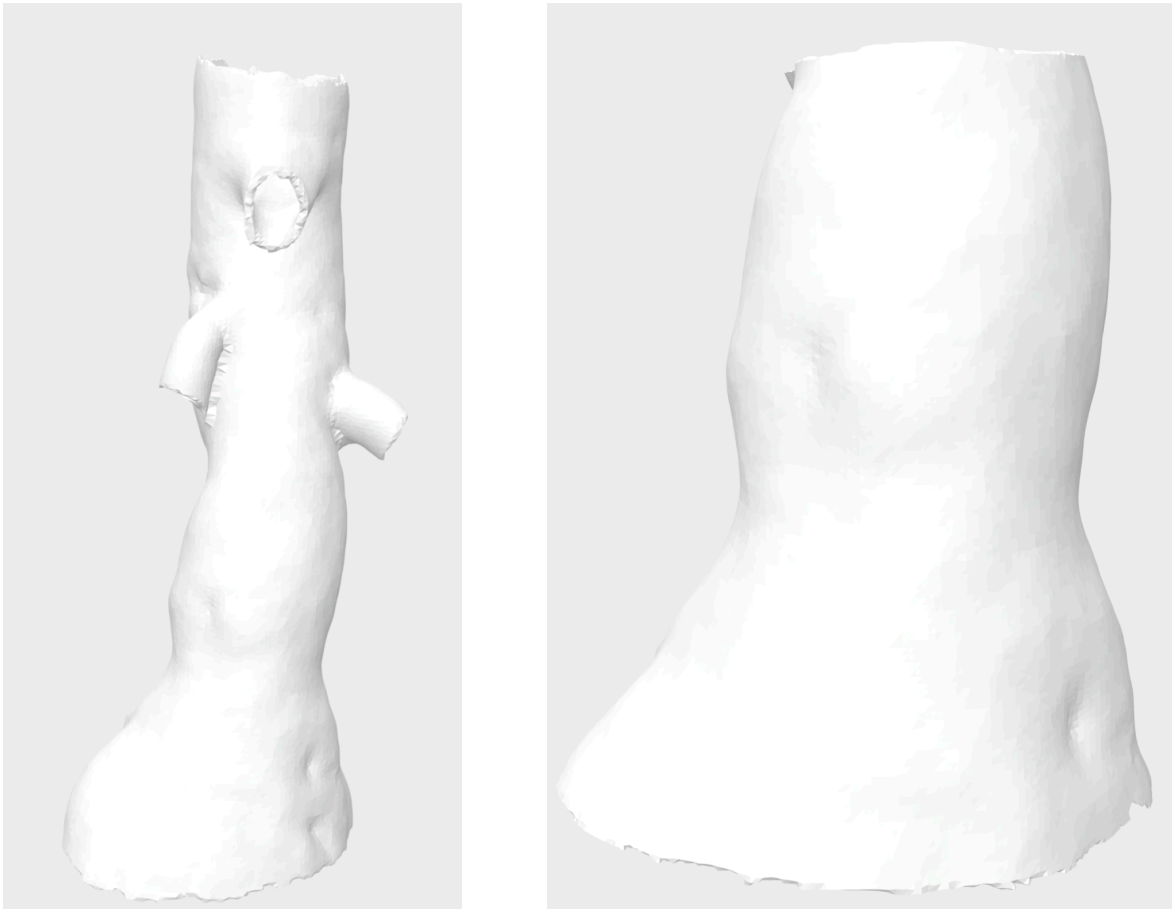

Figure 15: Aortic neck part of the segmentation, used for the aorta models and stent graft models. Left: the aortic neck and the branches of the renal arteries and superior mesenteric artery. Right: the aortic neck (infra-renal part). This part is important for measurements and sealing.

Table 7: Morphology and stent diameters of the selected subjects. The straight stent diameter is the diameter of the used stent graft during EVAR procedure for this patient. The maximal diameter of the aorta is the largest measured diameter in the segmentation and the maximal diameter of the personalized stent graft is the largest measured diameter in the 3D model of the personalized stent graft.

	Morphology	Max diameter aortic neck (mm)	Straight stent diameter (mm)	Personalized stent max (mm)
Subject 1	Straight, infra-renal	26	28	28
Subject 2	Curve, Infra-renal	22	25	25
Subject 3	Curve, tapered Infra-renal	27	36	29
Subject 4	Straight, infra-renal	27	36	30
Subject 5	Straight, Infra-renal (short neck)	25	28	27

PRINTING

First research was done to the properties of the materials of the stent grafts and the aorta and to the available materials at the printing labs of the University of Twente.

AORTA MODEL

We need a flexible and strong material, which would not tear when a stent graft is placed inside the model. Different materials are considered but only two materials are tested for printing the aorta models.

First, we printed aorta models in elastic resin with the FORM2 printer. This printer uses stereolithography (SLA) technique and is capable of printing detailed models. Elastic resin is a very flexible and soft material, has a tensile strength of 3.23 MPa and is often used in medical models for simulation.[46] We tested two aorta models and both models shown problems with printing. Some tears are visible (Figure 16) and it was not possible to complete the printing process.

Figure 16: Aorta models printed in elastic resin. On the left, an aorta with the branches of the renal arteries, the complete aneurysm and bifurcation to the iliac arteries are shown. On the right, an upper part of the aorta and aneurysm can be seen, including the branches of the renal arteries and superior mesenteric artery. In the aortic neck and upper part of the aneurysm, tears are visible.

Secondly, we printed the aortas with Agilus30 and the Stratasys ObJet260 Connex3 printer. Agilus30 is a flexible material and has a tensile strength of 2.4 – 3.1 MPa and a Young's Modulus of 0.6 MPa.[47,48] Printing the aorta models in Agilus30 is a time-consuming (1-2 days) process but results in usable aorta models (Figure 17). After stenting the aorta models with a 1 mm and 1.5 mm wall thickness, they rupture and are considered not suitable for further measurements. We only used the 2 mm wall thickness for further research. [45]

Figure 17: Aortic neck model, one of the first prints.

STENT GRAFTS

Various materials were discussed and tested. In Table 8, the different material properties of the used materials can be seen. We can conclude from this table that the material properties are different than the properties of nitinol and there is no preference material. Therefore, we tested the various materials with different properties.

Table 8: Material properties of nitinol and available and tested 3D print materials.

	Nitinol-55 [43]	Nitinol + PET graft [49]	NinjaFlex [50]	FlexiFil [51]	Flex 45 [52]	Cheetah [53]
Youngs Modulus (MPa)	70	-	12	95	95	26
Yield strength (MPa)	103-138	4.6	4	-	-	9
Tensile strength (MPa)	860	59.3	26	24	24	39
Strain at break	-	-	660% (elongation at break)	530% (elongation at break)	530% (elongation at break)	580% (elongation at break)

The first stents were printed with NinjaFlex and the Ultimaker3 printer. We concluded that NinjaFlex was not as flexible as expected and the straight printed stents were difficult to position in the printed aorta (Figure 18).

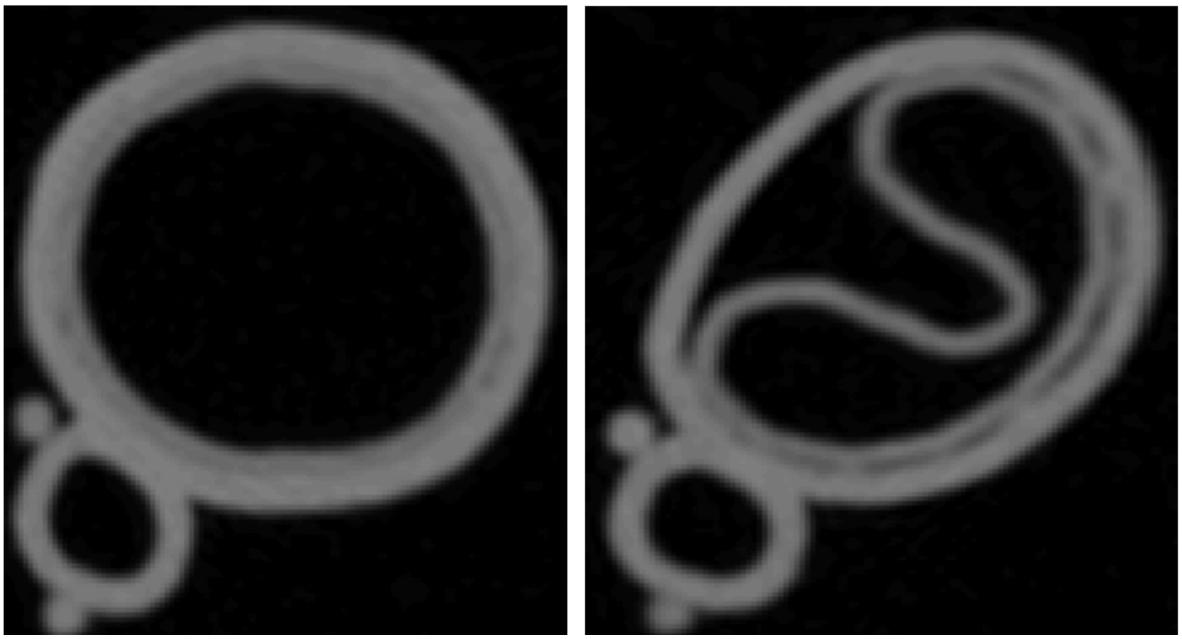

Figure 18: CT-scan of the printed stent grafts in NinjaFlex placed in the aorta model. Left: transversal slice of the aorta model with the personalized stent graft and a good sealing. Right: transversal slice of the aorta model with the straight stent graft, which could not unfold and bad sealing is seen at the unfolded side of the stent graft.

Flexifil and Flex45 have similar material properties and are smart memory polymers, which gives these materials comparable properties as nitinol. Flexifil and Flex45 are known as flexible and strong materials and can be folded even when printed in complicated forms. However, only Flex45 was available and we printed five straight stent and personalized stents with this material and the Ultimaker3 printer. The printer was not able to print more than 1-2 cm in height with this material, due to unknown reasons. Small parts of straight stents, as shown in Figure 19, are flexible and easily foldable. However, we were not able to use this material for further research.

Figure 19: Small part of straight stents printed with Flex45.

Finally, we printed the stent grafts with Cheetah and the Ultimaker3 printer. It has a higher Young's modulus and tensile strength, but when we adjust the wall thickness it could be more flexible. The printed stents were flexible and foldable, although less than expected. Also, we printed straight stents in a different geometry, and meshes were created in the straight stents to make them more flexible. We were not able yet to print the personalized stent graft in the geometry with meshes. We use these stents for the distention measurements.

STRAIGHT VERSUS PERSONALIZED

Different methods to measure the distention of the aorta and calculate the force on the aortic wall are created and tested. The aorta models are scanned with an Iluma Cone Beam CT-scanner (Imtec Imaging, Ardmore OK, USA).

First, we tried to measure the distention by adding spheres on the outside of the aorta model (Figure 20) as markers. However, there were difficulties distinguish the spheres from the aortic wall in the obtained CT-scans, due to comparable HU of the aorta and spheres.

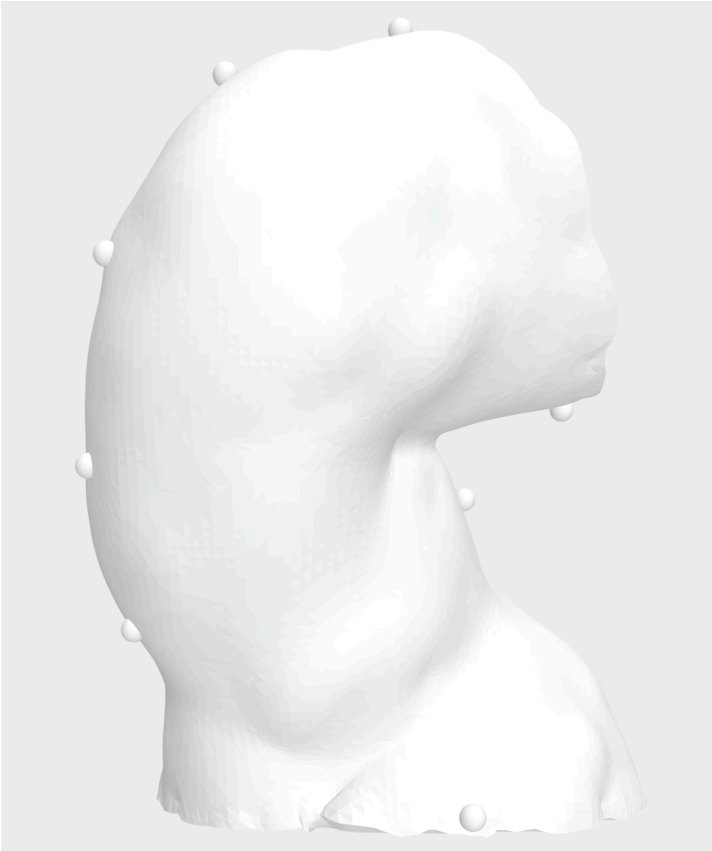

Figure 20: Aorta model with spheres. The displacement of the spheres is measured and this is used to calculate the distension of the aortic wall in the models when a stent graft is placed.

Secondly, we printed the aorta model (without markers) and glued spheres on the outside of the aorta model (Figure 21 and 22). It can be seen in Figure 22 that the markers are visible but nearly have the same intensity (HU) as the aorta model, which makes it complicated to distinguish the markers from the aorta and therefore this method not met the requirements and is not used for further measurements.

Figure 21: Aorta model with different materials for testing.

Figure 22: CT-scan of the marked aorta with the test spheres. From left to right: transversal, coronal and sagittal plane.

Thirdly, we tested a method using metal wires instead of the spheres (Figure 23). On the CT-scans the metal wires are clearly visible and easy to distinguish from the aorta. Therefore, we used this method for further measurements and different CT-scans were made.

Figure 23: Aorta model with metal wires.

STRAIGHT STENT GRAFTS

The printed solid stent grafts were not easily foldable. Therefore, the straight stent grafts were printed in a mesh structure. This resulted in more flexible stent grafts compared with the solid straight stent grafts and the personalized stent grafts. However, these meshed straight stent grafts stay folded in the aorta as shown in Figure 24 and 25. No aortic wall distention can be measured, and no further measurements can be done with these scans.

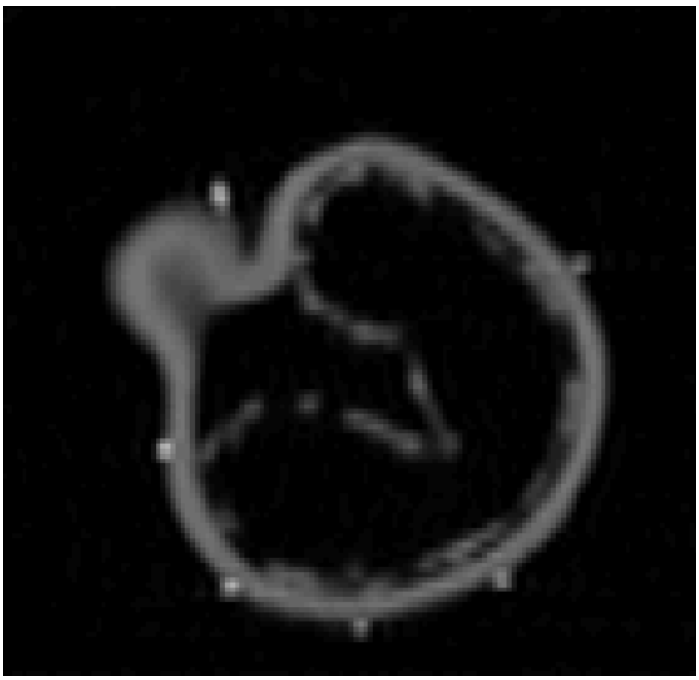

Figure 24: Transversal slice of the aorta model with a straight stent graft. The stent graft is not able to completely unfold in the aorta.

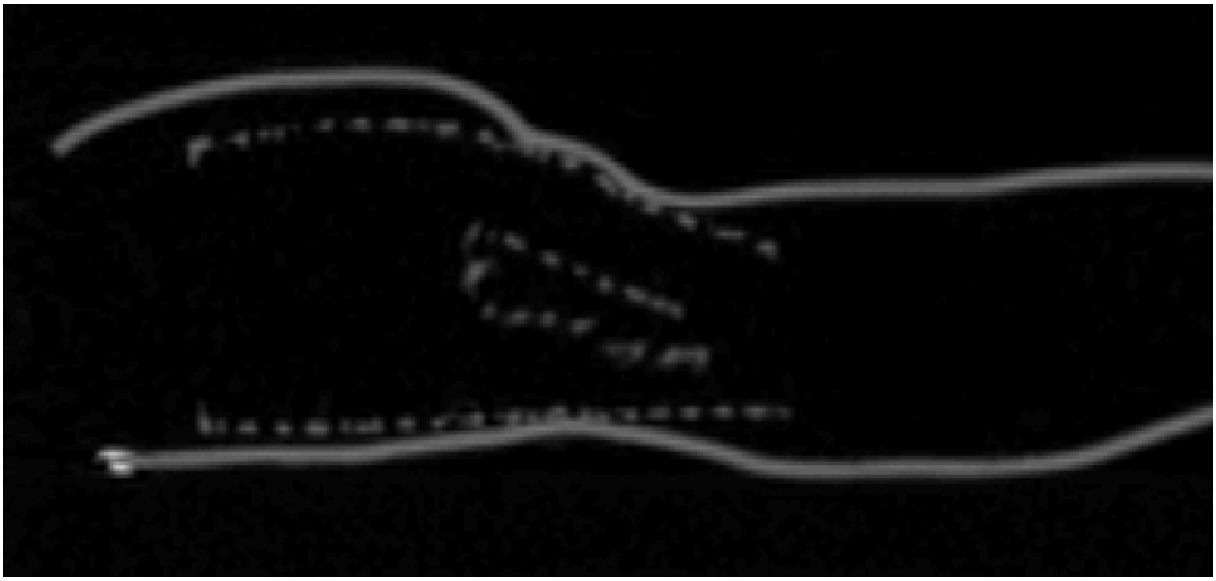

Figure 25: Aorta model with a straight stent graft. Two "legs" are visible, which are created by the fold in the stent graft. Also, in these scans no distention of the aortic wall is apparent.

PERSONALIZED STENT GRAFTS

The personalized stent graft shows a good or mediocre sealing and a little distension of the aorta, created due to the oversizing of the stent graft (10%). For some other personalized stent grafts, it was difficult to place them in the aorta model, when the stent graft was not flexible enough. In the figures below (Figure 26 and 27), a personalized stent graft is visible in the aorta model.

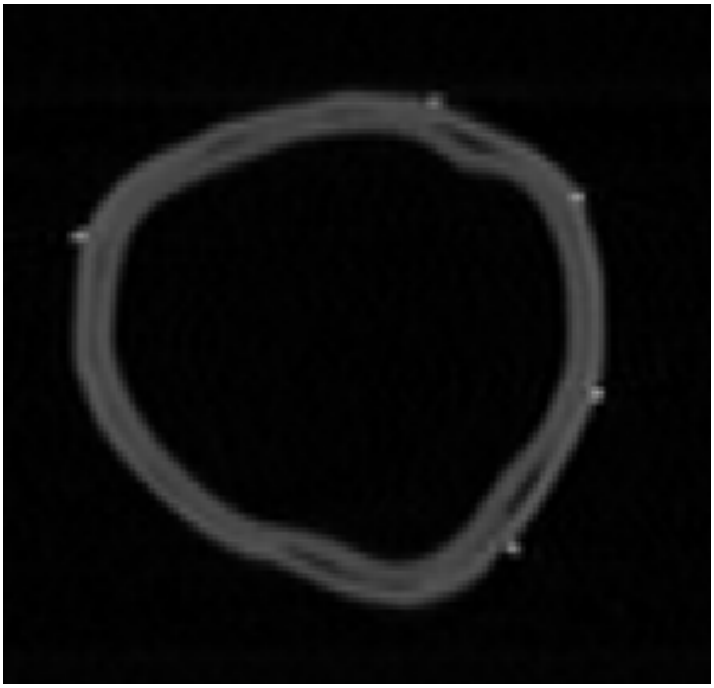

Figure 26: Transversal slice of the aorta model with metal wires visible as white dots.

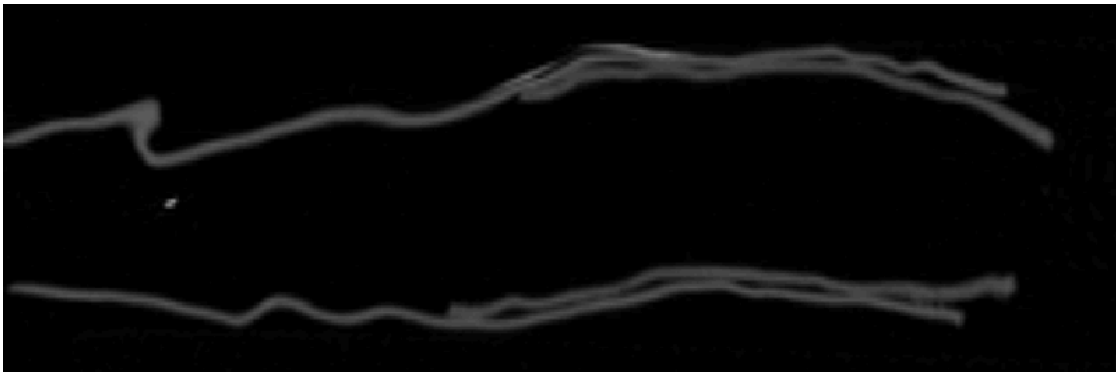

Figure 27: Personalized stent graft placed in the aorta model. Sealing is not perfect, due to difficulties placing the stent.

NITINOL STENT GRAFT

To compare with the real-life situation, we scanned an aorta model with a nitinol stent graft (Figure 28 and 29). In the transversal scans, with the nitinol stent graft, small gutters can be seen. With our measurement method no distention of the aortic wall is measurable when the nitinol stent graft is used. The pressure caused by the nitinol stent is smaller than for the personalized stent graft in these models.

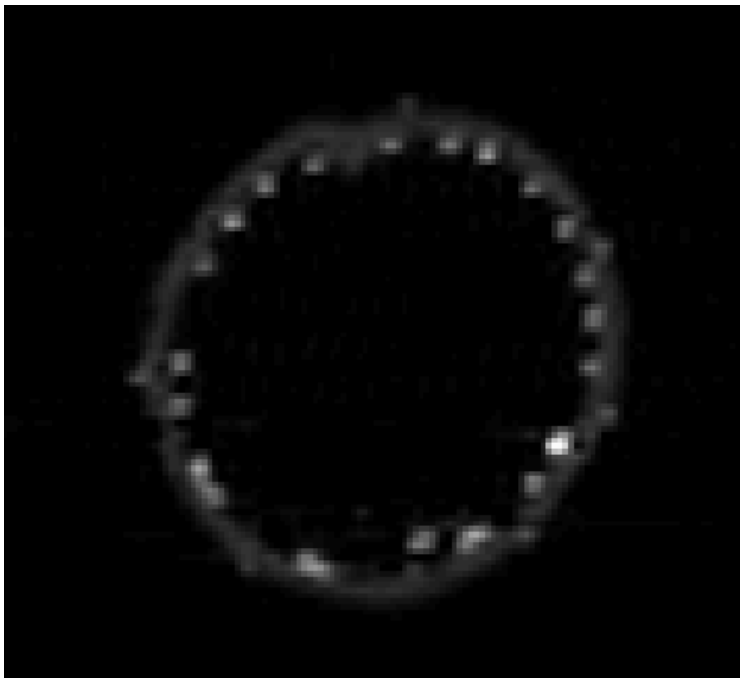

Figure 28: Transversal slice (CT-scan) of the aorta model with the nitinol stent.

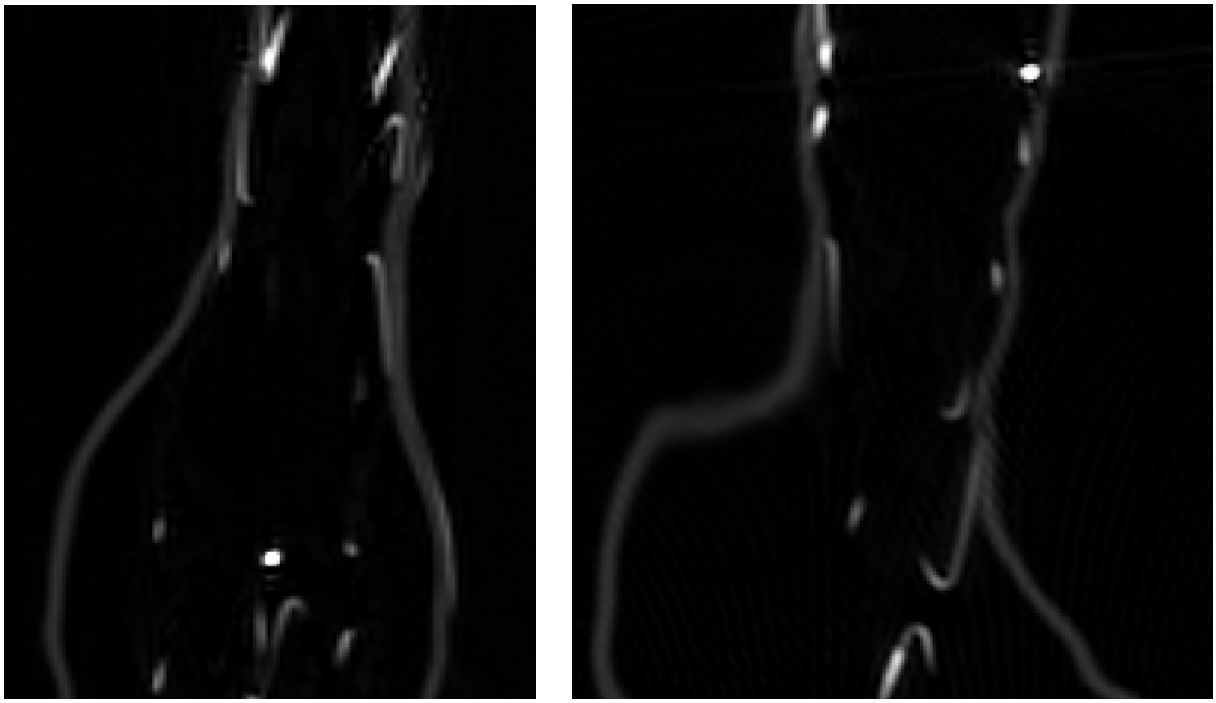

Figure 29: CT-scan of the aorta model with the nitinol stent. Left: coronal slice. Right: Sagittal slice.

DISCUSSION

This research has investigated the effect of straight stent grafts versus personalized stents. First, a segmentation method was created that obtained the required properties of the aneurysm and aorta. Secondly, different materials were discussed for 3D printing the aorta and stent grafts. The material used for the aorta models is a promising material, but the stent graft material is not comparable with the real-life situation. Additionally, a measurement method was created to compare the aortic wall distention for a straight stent graft and a personalized stent graft. For both types of stent grafts we were not able to measure differences in aortic wall pressure, however, in some cases better sealing was seen with some personalized stent grafts.

SEGMENTATION

The semi-automatic segmentation method created in this research is still suboptimal, and occasionally the kidneys and spine are included in the segmentation which needed to be removed manually in Meshmixer. A segmentation method that only segment the aorta and the aneurysm in all patients is preferred.

Furthermore, the segmentation method was limited in identifying calcifications and thrombi from the aortic wall in some cases, and only the part where blood flow was visible in the CTA scans were segmented. For this research, it was not a drawback because we only used the volume containing the aortic neck and after checking the segmentations of the included patients it was seen that there were no significant abnormalities such as calcifications to take into account for 3D printing the aorta models. For further research, the segmentation method should be adapted in such a way the differentiation between the aortic wall, the blood flow, calcifications and thrombi should be possible.

PRINTING

The materials used for printing are not ideal. For further research, different materials should be considered, which are more suitable and show similar material properties as the aorta and the nitinol stent grafts.

AORTA

We tested two materials, elastic resin and Agilus30. These materials are the most flexible materials available at the printing labs at University of Twente. First, we make test prints with the elastic resin, but due to printing problems as can be seen in Figure 16, these models were not usable for further measurements. Agilus30 was suitable and met our requirements and this material is used for 3D printing the aorta models. Further research to different materials may be required for the following steps in this research (see appendix).

The wall thickness of the abdominal aorta is approximately 1.5 mm and therefore we tested 1 mm, 1.5 mm and 2 mm wall thickness for our models. The 3D printed models with a wall thickness of 1 mm and 1.5 mm were not strong enough and teared, also due to the stiff material of the stent grafts. For further research, when a better material and more representative stent graft is available the aortic wall thickness needs to be taken into account.

STENT GRAFTS

Different stent graft materials are tested in this research. Flexifil and Flex45 are promising materials with good material properties, comparable with nitinol. We were not able to 3D print the stent grafts in these materials and further research is required. The NinjaFlex stents were not as flexible as expected, which makes folding of the solid stent graft difficult. This resulted in an unfolded straight stent graft in the aorta model and big gutters were visible as seen in Figure 18 and 24. These models and scans were not suitable for measuring the aortic wall distention.

The second tested material described, Cheetah, was not as flexible as thought and the solid stent grafts were not easily foldable which make it difficult to place the stent graft in the aorta model. When printed in a different geometry (meshed), the stent is more flexible and showed similar behavior as the nitinol stent graft. The stent grafts printed in NinjaFlex or Cheetah are in solid form too stiff and in mesh structure too flexible. We were not able to measure any distention differences of the aortic wall between the personalized stent grafts and the straight stent grafts. Further research to the possibilities of 3D printing in different materials and geometrical designs is required and a different measuring method should be considered to obtain information about the aortic wall distension. Also computer models can be useful for further research to different materials and stent graft geometries.

STRAIGHT VERSUS PERSONALIZED MEASURING METHOD

At first attempt of measuring the aortic wall distension, we used spheres (Figure 20). However, these markers are made from comparable material as the aorta models, because the spheres need to be printed at the same time in the same printer. Therefore, only different compositions of the materials with that specific printer can be used. This results in difficulties distinguish the spheres from the aortic wall in the CT-scans made, due to little differences in HU of the aortic wall and spheres.

Secondly, we printed the aorta model without the markers and glued spheres of different sized and materials on the outside of the aorta and made a test CT-scan (Figure 21 and 22). It can be seen in Figure 22 that the different spheres are visible but nearly have the same HU as the aorta model, which makes it complicated to distinguish the markers from the aortic wall. Besides, the spheres were influencing the shape and deforming of the aortic wall when they were placed in a notch or in the angulation of the aortic model. This method is also not used for further measurements.

Finally, we used metal wires instead of spheres. It was easier to from the wires to the complex shape of the aorta model and the wires were thinner (<1 mm) and not influencing the aorta and the shape change of the aorta when a stent graft was placed (Figure 23). On the CT-scans the metal wires are clearly visible. The metal wires have a higher HU, resulting in the fact that they can easily distinguished from the aortic wall and therefore these were used for further measurements. When the HU are used for segmentation, the wires could be easily segmented from the aortic models and the distention of the aortic wall can then be viewed and calculated automatically. This can be done by determining the central lumen line (CLL) in the aorta models and when the distance from the CLL to the metal wires is calculated in the three scans, the distention of the aortic wall can be calculated.

Nevertheless, placing the metal wires is a time-consuming and secure task. The wires need to be placed on a specific place, with a particular distance from each other. The wires should be placed from top to bottom of the aorta model and with a determined distance from each other. For this study, we placed the wires approximately 0.5 - 1 cm from each other. Different distances should be considered to obtain

the best results for distension measurements. The wires were clearly visible, and it would be possible to decrease the distance to 0.5 cm or smaller.
Further research to possible materials is required to obtain more (and better) results in this part of the research. Also, a different method for placing the stent grafts should be considered, like a delivery system used in EVAR procedures.

The personalized stent grafts give better sealing results in this research. In Figure 18 and in Figure 24 a transversal slice of a CT-scan with the personalized stent grafts in NinjaFlex and Cheetah are visible, and in these figures a moderate/good sealing can be seen between the aortic wall and personalized stent graft. Compared to Figures 18 (right) and 24, where the transversal slice of the CT scans of the straight stents are visible, a lousy sealing can be seen. This may be a good indication of a better sealing with the personalized stent grafts; however, no conclusions can be made from these results, more measurements should be done and more research is required.

In vivo, the blood pressure is also an important factor for the sealing of the stent graft. In these models and test we did not take the blood pressure into account. For further research the blood pressure and flow should be considered.

STRAIGHT STENT GRAFT

The straight stent grafts in the mesh structure were flexible and foldable, however the stent was unable to completely unfold in the aorta model. This results in a lousy sealing and no aorta distension could be measured for these stents. In Figure 24 it can be seen that the diameter of the stent graft is too large, which is due to the oversizing, and makes it impossible to unfold completely.

PERSONALIZED STENT GRAFT

The used materials for the personalized stent grafts, NinjaFlex and Cheetah, were not flexible enough. It was difficult to place the stent grafts in the aorta mode and it was not possible to place the personalized stent grafts in all models. In the other model we saw a mediocre/good sealing and a little aortic wall distension. However, the sealing was not good enough and still some gutters can be seen in some cases as shown in Figure 26.

NITINOL STENT GRAFT

We tested and scanned an off-the-shelf nitinol stent graft. In these models no aortic wall distension could be measured and the oversizing with this stent graft causes no aortic neck dilatation. In some spots an incomplete sealing was visible on the CT-scan. However, the graft material is also responsible for the sealing and is not (always) visible on the CT-scan and therefore no conclusions can be made from these results.

IMAGING

The CTA scans were made without knowledge at what point of the cardiac cycle the images were taken and if we measure the maximum aorta diameter. Several studies show increase in aortic neck diameter during the cardiac cycle. The maximum aorta diameter, during systole, should be used for determining the stent graft diameter. Otherwise, the aortic neck diameter may become greater than the stent graft diameter and migration of the stent graft could occur. By using ECG gated CTA scans, we can measure the different diameters during the cardiac cycle and obtain the maximum aorta diameter to improve the fit of the personalized stent grafts. [22,31,54]

CONCLUSION

In this thesis we explore the possibilities of 3D printing endovascular stent grafts and evaluate the personalized stent graft. A semi-automatic segmentation method is created which is suitable for the aortic neck segmentation, but further work is required for a whole aneurysm segmentation. 3D models of 39 patients were made and five of these models were selected for 3D printing. The aortas were printed in Agilus30 with a wall thickness of 2 mm and the stent grafts were printed in NinjaFlex and Cheetah. We hypothesized that personalized stent grafts provide a better sealing with less stress on the aortic wall and therefore could reduce the risk of complications such as endoleak. The straight and personalized stent grafts applied not as much pressure on the wall as thought and we were unable to perform good measurements, but an inadequate sealing was seen for some straight stent grafts. The results showed that a better sealing could be obtained by using personalized stent grafts in our aorta models, however the used materials for the 3D printing of the stent grafts are not comparable with the nitinol stent graft and therefore more research is required.

REFERENCES

1. Reimerink JJ, Hoornweg LL, Vahl AC, et al. Endovascular repair versus open repair of ruptured abdominal aortic aneurysms: A multicenter randomized controlled trial. *Ann Surg*. 2013;258(2):248-256.

2. Rubin R., Strayer D., Rubin E. MJ. *Rubin's Pathology: Clinicopathologic Foundations of Medicine*. Vol 45. 5th ed. Lippincott Williams & Wilkins; 2008.

3. Sakalihasan N, Michel JB, Katsargyris A, et al. Abdominal aortic aneurysms. *Nat Rev Dis Prim*. 2018;4(1).

4. Boron WF, Boulpaep EL. *Medical Physiology*. 2nd ed. Elsevier Health sciences; 2012.

5. Rucińska Z, Juzwiszyn J, Bolanowska Z, et al. The evaluation of the postoperative course in patients operated due to abdominal aortic aneurysm as urgent or elective procedure. *Pol Przegl Chir*. 2018;90(6):1-5.

6. St. George Institute of Aortic Aneurysm & Aortic Valve Disease. Aortic aneurysm. http://aortainstitute.co.uk/conditions-and-diseases/aortic-aneurysm/. Published 2019. Accessed February 4, 2019.

7. Keisler B, Carter C. Abdominal Aortic Aneurysm. *Am Fam Physician*. 2015;91(8):538-543.

8. Sakalihasan N, Limet R, Defawe OD. Abdominal Aortic Aneurysm. *Lancet*. 2005;365(April 30):1577-1589.

9. Forsdahl SH, Singh K, Solberg S, Jacobsen BK. Risk factors for abdominal aortic aneurysms: a 7-year prospective study: the tromsø study, 1994 2001. *Circulation*. 2009;119(16):2202-2208.

10. Nordon IM, Hinchliffe RJ, Loftus IM, Thompson MM. Pathophysiology and epidemiology of abdominal aortic aneurysms. *Nat Rev Cardiol*. 2011;8(2):92-102.

11. Gunnarsson K, Wanhainen A, Djavani Gidlund K, Björck M, Mani K. Endovascular Versus Open Repair as Primary Strategy for Ruptured Abdominal Aortic Aneurysm: A National Population-based Study. *Eur J Vasc Endovasc Surg*. 2016;51(1):22-28.

12. Hoornweg LL, Wisselink W, Vahl A, Balm R. The Amsterdam Acute Aneurysm Trial: Suitability and Application Rate for Endovascular Repair of Ruptured Abdominal Aortic Aneurysms. *Eur J Vasc Endovasc Surg*. 2007;33(6):679-683.

13. Pejcic S, Ali Hassan SM, Rival DE, Bisleri G. Characterizing the mechanical properties of the aortic wall. *Vessel Plus*. 2019;2019:1-12.

14. The Johns Hopkins University, The Johns Hopkins Hospital and TJHHSC. Abdominal Aortic Aneuysm. https://www.hopkinsmedicine.org/health/conditions-and-diseases/abdominal-aortic-aneurysm. Accessed March 19, 2019.

15. Prinssen M, Verhoeven ELG, Buth J, et al. A Randomized Trial Comparing Conventional and Endovascular Repair of Abdominal Aortic Aneurysms. *N Engl J Med*. 2004;351(16):1607-1618.

16. Droc I, Raithel D, Calinescu B. Abdominal Aortic Aneurysms - Actual Therapeutic Strategies. In: *Aneurysm*. InTech; 2012.

17. Kansagra K, Kang J, Taon M-C, et al. Advanced endografting techniques: snorkels, chimneys, periscopes, fenestrations, and branched endografts. *Cardiovasc Diagn Ther*. 2018;8(S1):S175-S183.

18. Stavropoulos SW, Charagundla SR. Imaging Techniques for Detection and Management of Endoleaks after Endovascular Aortic Aneurysm Repair. *Radiology*. 2007;243(3):641-655.

19. Kassem TW. Follow up CT angiography post EVAR: Endoleaks detection, classification and management planning. *Egypt J Radiol Nucl Med*. 2017;48(3):621-626.

20. Mastracci TM. Fenestrated endografts for complex abdominal aortic aneurysms. *Perspect Vasc Surg Endovasc Ther*. 2010;22(4):214-218.

21. Droc I, Droc G, Buzila C, Calinescu FB. Abdominal Aortic Aneurysms (AAA): Actual approach actual approach. In: *New Approaches to Aortic Diseases from Valve to Abdominal Bifurcation*. Elsevier Inc.; 2018:393-402.

22. Belvroy VM, Houben IB, Trimarchi S, Patel HJ, Moll FL, Van Herwaarden JA. Identifying and addressing the limitations of EVAR technology. *Expert Rev Med Devices*. 2018;15(8):541-554.

23. Wang T, Zhao J, Yuan D, et al. Comparative effectiveness of open surgery versus endovascular repair for hemodynamically stable and unstable ruptured abdominal aortic aneurysm. *Med (United States)*. 2018;97(27):14-19.

24. Stather PW, Sidloff D, Dattani N, Choke E, Bown MJ, Sayers RD. Systematic review and meta-analysis of the early and late outcomes of open and endovascular repair of abdominal aortic aneurysm. *Br J Surg*. 2013;100(7):863-872.

25. Morgan NB. Medical shape memory alloy applications - The market and its products. *Mater Sci Eng A*. 2004;378(1-2 SPEC. ISS.):16-23.

26. Raptis A, Xenos M, Spanos K, Kouvelos G, Giannoukas A, Matsagkas M. Endograft Specific Haemodynamics After Endovascular Aneurysm Repair: Flow Characteristics of Four Stent Graft Systems. *Eur J Vasc Endovasc Surg*. 2019;58(4):538-547.

27. Patel R, Sweeting MJ, Powell JT, Greenhalgh RM. Endovascular versus open repair of abdominal aortic aneurysm in 15-years' follow-up of the UK endovascular aneurysm repair trial 1 (EVAR trial 1): a randomised controlled trial. *Lancet*. 2016;388(10058):2366-2374.

28. De Bruin JL, Baas AF, Buth J, et al. Long-term outcome of open or endovascular repair of abdominal aortic aneurysm. *N Engl J Med*. 2010;362(20):1881-1889.

29. Schanzer A, Simons JP, Flahive J, et al. Outcomes of fenestrated and branched endovascular repair of complex abdominal and thoracoabdominal aortic aneurysms. In: *Journal of Vascular Surgery*. Vol 66. Mosby Inc.; 2017:687-694.

30. Malas MB, Hicks CW, Jordan WD, et al. Five-year outcomes of the PYTHAGORAS U.S. clinical trial of the Aorfix endograft for endovascular aneurysm repair in patients with highly angulated aortic necks. *J Vasc Surg*. 2017;65(6):1598-1607.

31. Kouvelos GN, Oikonomou K, Antoniou GA, Verhoeven ELG, Katsargyris A. A Systematic Review of Proximal Neck Dilatation after Endovascular Repair for Abdominal Aortic Aneurysm. *J Endovasc Ther*. 2017;24(1):59-67.

32. Medtronic. *Endurant ™ II Endurant ™ IIs*. http://manuals.medtronic.com/content/dam/emanuals/cardio/M059211T001_Rev1A_view.pdf.

33. Droc I, Calinescu FB, Droc G, Blaj C, Dammrau R. Aortic stenting. *Minim Invasive Ther Allied Technol*. 2015;24(5):296-304.

34. Boers T. Personalized endovascular stent grafts. 2017.

35. Boers T. M3Dical printing of custom-made stents. 2016.

36. Singh C, Wong C, Wang X. Medical Textiles as Vascular Implants and Their Success to Mimic Natural Arteries. *J Funct Biomater*. 2015;6(3):500-525.

37. Santos ICT, Rodrigues A, Figueiredo L, Rocha LA, Tavares JMRS. Mechanical properties of stent-graft materials. *Proc Inst Mech Eng Part L J Mater Des Appl*. 2012;226(4):330-341.

38. Kamila S. Introduction, classification and applications of smart materials: An overview. *Am J Appl Sci*. 2013;10(8):876-880.

39. Kleinstreuer C, Li Z, Basciano CA, Seelecke S, Farber MA. Computational mechanics of Nitinol stent grafts. *J Biomech*. 2008;41(11):2370-2378.

40. Li Q, Zeng Y, Tang X. The applications and research progresses of nickel-titanium shape memory alloy in reconstructive surgery. *Australas Phys Eng Sci Med*. 2010;33(2):129-136.

41. Meier H., Haberland C., Frenzel J. Structural and functional properties of NiTi shape memory alloys. *Innov Dev Virtual Phys Prototyp*. 2012:291-296.

42. Dadbakhsh S, Speirs M, Kruth JP, Schrooten J, Luyten J, Van Humbeeck J. Effect of SLM parameters on transformation temperatures of shape memory nickel titanium parts. *Adv Eng Mater*. 2014;16(9):1140-1146.

43. Whittaker DR, Fillinger MF. The engineering of endovascular stent technology: A review. *Vasc Endovascular Surg*. 2006;40(2):85-94.

44. Lang RM, Cholley BP, Korcarz C, Marcus RH, Shroff SG. Measurement of regional elastic properties of the human aorta: A new application of transesophageal echocardiography with automated border detection and calibrated subclavian pulse tracings. *Circulation*. 1994;90(4 I):1875-1882.

45. Schoffelen FWT. *Towards 3D-Printed Personalized Stent Grafts : Comparing Straight with Personal Stent Graft Design In Infrarenal Neck of Abdominal Aortic Aneurysm*.; 2019.

46. Formlabs. Elastic Elastic Resin for Soft Flexible Parts. 2019. https://formlabs-media.formlabs.com/datasheets/Elastic_Resin_Technical.pdf.

47. Stratasys. Agilus30, polyjet rubber-like material properties. 2018.

48. Stratasys. Digital Materials (DMs) Data Sheet. 2013. http://stratasys.com/materials/polyjet/digital-materials.

49. Kleinstreuer C, Li Z. Analysis and computer program for rupture-risk prediction of abdominal aortic aneurysms. *Biomed Eng Online*. 2006;5.

50. NinjaTek. NinjaFlex ® 3D Printing Filament: Flexible Polyurethane Material for FDM Printers. 2016

51. FormFutura. FlexiFil 3D printing filament, Technical data sheet. 2016.

52. Mcpp. Flex 45. 2015.

53. NinjaTek. NinjaTek, Cheetah. https://ninjatek.com/products/filaments/cheetah/

54. van Herwaarden JA, Bartels LW, Muhs BE, et al. Dynamic magnetic resonance angiography of the aneurysm neck: Conformational changes during the cardiac cycle with possible consequences for endograft sizing and future design. *J Vasc Surg*. 2006;44(1):22-28.

55. Powell A, Kashyap VS. Design and Clinical Considerations for Endovascular Stent Grafts. *Interv Cardiol Clin*. 2016;5(3):381-389.

56. Katzen BT, MacLean AA. Complications of endovascular repair of abdominal aortic aneurysms: A review. *Cardiovasc Intervent Radiol*. 2006;29(6):935-946.

57. Rodrigues A, Figueiredo L, Bordado J. Abrasion behaviour of polymeric textiles for endovascular stent-grafts. *Tribol Int*. 2013;63:265-274.

58. Smeds MR, Charlton-Ouw KM. Infrarenal endovascular aneurysm repair: New developments and decision making in 2016. *Semin Vasc Surg*. 2016;29(1-2):27-34.

59. Groot Jebbink E, Goverde PCJM, van Oostayen JA, Reijnen MMPJ, Slump CH. Innovation in aortoiliac stenting: an in vitro comparison. *Med Imaging 2014 Image-Guided Proced Robot Interv Model*. 2014;9036:90361X.

APPENDIX 1

FURTHER RESEARCH

SEGMENTATION

A segmentation method that only segment the aorta and the aneurysm in all patients is preferred. The method used in this research have some limitations, regarding the identification of calcifications and thrombi from the aortic wall in some cases. For further research, a more secure and detailed method is required. Also, the possibilities of artificial intelligence (AI) and the creation of a network for segmentation could be investigated.

In this part of the research we do not consider the blood pressure and flow. The process of determining the size and shape of the stent graft could be optimized when we consider the blood pressure in the aorta. By using ECG gated CTA scans, we, first of all, can measure the difference in aorta diameter during diastole and systole (% change in diameter) and study the pressure and flow more specific in the aortic neck and the aneurysm. The change in aorta diameter can be used for oversizing the stent graft and this decreases the change in over- or under-sizing the stent graft, which reduces the change of complications after surgery, such as endoleak and migration of the stent graft.

PRINTING

Besides different materials also different geometries should be tested. Previous research in the Meander Medical Center has shown that Z-shaped and circular shaped stent geometries offer balanced characteristics, where the most important factors were good 3D printability and anatomically shape-able properties.[34] For further research these geometries should be considered in the personalized stent grafts.

GRAFT MATERIAL

We have not looked into possible graft materials. When we can print nitinol or a material with similar properties, further research on possible graft materials is required. The production of a graft requires precision. In previous research different techniques are proposed, dissolving polymer and melting polymer. Groot Jebbink et al. produced a set up using a heated bath with a bowl inside in which the graft material is dissolved and in which the stent is submersed. This resulted in a covered stent with a flexible graft. [59]

In previous research polyurethane is used, which also comes in a biocompatible form. This material is already used in stent grafts and therefore this set up might be interesting to produce a graft for the personalized stent grafts. Tim Boers investigated this method and produced a test stent with graft with feasible results. [35] He concluded that the graft material could not bridge some gaps long enough to be able to evaporate all the water and solidify. However, this can be improved by adjust the coating method and add more material (carbothane) to create a more viscous solution.

Secondly, Ultra-High molecular weight polyethylene (UHWMPE) might be a suitable graft material. This is a biocompatible polymer and shows high impact strength, good wear resistance and fatigue resistance. UHWMPE promoting better or equal healing and elicit fewer inflammatory responses, compared with polyesters. UHWMPE is self-lubricant and very smooth and slippery devices can be

created, due to its low friction coefficient and non-stick surface. These properties make UHWMPE a suitable candidate as graft material. It is a thermoplastic and therefore is not dissolved but molten to allow processing. [34,35,37]

AORTA PHANTOM – TEST SET UP

To study the influence of the blood pressure and flow on the aortic wall, the sealing of the stent graft and aortic wall and on the stent graft (personalized and off-the-shelf) a more detailed research is required. Therefore, an aorta model and test set up can be made. Requirements for this set up are:

- The aortic model is comparable with the in vivo aorta
- The thrombi and calcifications should be taken into account
- Stent grafts can be placed in the aortic aneurysm
- Understanding of the biological composition and biomechanics of the vascular system is wanted
- A pulsatile waveform can be simulated
- Different blood pressures can be simulated
- Flow can be measured
- Pressure on the aortic wall can be measured

APPENDIX 2

LIST OF REQUIREMENTS

This list of requirements is made in previous research by Tim Boers and formed based upon literature and personal communication.[34] The requirements are subdivided into four categories; functional, operational, technical, and transitional requirements.

FUNCTIONAL

- Should be able to be used for either all abdominal aneurysms or at least one of the following: infra-, juxta- and supra-renal abdominal aneurysms.
    - Stent graft should include branches or fenestrations for renal and visceral arteries.
    - Should also be used for infra-renal aneurysms with a small aortic neck.
- Should be inserted via the femoral artery.
    - Compatible with guide wires.
    - Profile lower than 20 French (or smaller). [55]
- Should have a user interface similar or more intuitive to current EVAR products.
    - Positioning via radiopaque beads should indicate locations of top and bottom as well as fenestrations/branches.
    - Stent should be as radiopaque visible in its entirety as possible.
    - Should be able to be manipulated during placement.
    - Deployment should be controlled via rotating handles on the interface-end.
    - Should self-expand during deployment (SMA, SMP).
    - Should self-adhere to vessel wall through COF (chronic outward force) and RRF (radial resistive force) inherently in the stent.
- Custom made for better match with patient's anatomy
- Should be long enough to provide an artificial landing zone for subsequent sent grafts to be placed.
- Should be compatible with other brands of stent grafts as an artificial landing zone.

OPERATIONAL

- Should use angiographic images to produce data for use in the design of the stent graft.
- Should produce a 3D model of the stent graft in a file compatible with the AM (additive manufacturing) method (STL-file)
    - Should use a semi-automatic or automatic method to produce that model
- Should be produced with an 3D printing method.
    - Printer should be compatible with metal printing (Argon gas).
- Should have as low as possible material costs.
    - Should be capable to produce multiple products in the same manufacturing instance
- Should withstand post-processing annealing to ensure homogeneous material characteristics.
    - Nitinol requires annealing to ensure homogeneous super-elasticity and shape memory.
- Should be able to be covered with a polymer film.
    - Already certified and much used polymers: (e)PTFE and Dacron.
    - Interesting materials: PU and UWHMPE [37]

- Should prevent graft erosion and abrasion as much as possible. [37,56,57]
- Should be able to withstand a surface treatment for sterilization, both nitinol and the polymer. [37]

TECHNICAL

- Should have similar characteristics to conventional produced stent grafts.
    - Should comply with CE marking and FDA approved standards.
- Should have full patency longer than 2 years (comparison mid-term current devices). [58]
- Should cope with high alternating pressure inside the blood vessel.
    - Should have high endurance and little to no chance of breaking/fatigue.
- Should not induce to much aorta neck dilatation; COF should be balanced to ensure a proper seal, however, it should not cause unnecessary high wall stresses. with the vessel wall
- Should be flexible to retain profile without kinking; a high enough RRF should be ensured.
- Should allow for a polymer film to be created over the stent. Therefore space in between struts should be small.
- Should not migrate or leak.
    - Should be oversized by 10-20% to ensure good radial force, this should be in balance with potential vascular wall damage.
    - Should have a top stent with barbed wires to hook into the vessel wall.
    - Should have a graft design that prevents endoleak type III and IV.
- Should be biocompatible. [37]
    - Bio-inert towards blood.
    - Promote low vessel wall ingrowth.
    - Demote sclerotic plaque forming.
    - Low corrosion levels.
    - Should have a form of porosity or patterned holes for improved endothelialisation and increased flexibility.
    - Should not be toxic, allergic, or carcinogenic
    - Should not cause thrombosis, hemolysis, foreign body reaction or inflammatory response.

TRANSITIONAL

- Should reduce production time to less than one week from delivery of CTA scans.
- Should be placed as first stent graft to provide the operator with an artificial neck/landing zone.

APPENDIX 3

RESEARCH LINE

3D printing allows for three-dimensional freedom during production and gives the opportunity to use patient data allowing to produce patient specific products. 3D printing is a promising technique and has the protentional to reduce the production time and perhaps a reduction in post-operative complications.

The goal of the research project in Meander Medical Center is to develop a prototype personalized stent graft through 3D printing, which eventually can be tested in animals. The research is divided into three sub-foci: [34]

- Designing, fabricating, and grafting of a stent (including fenestrations when needed).
- Semi-automated method to extract dimensional data to match stent graft and patient anatomy
- Sterilization, packaging, and endovascular delivery of the stent graft.


Research into nitinol and 3D printing of nitinol (in combination with the production of a straight stent without graft).
Standardized tests should be performed to the characteristics of the conventional produced (laser-cut) nitinol.
Testing of a straight nitinol stent without graft.
Tests in tubular shape, charting its strengths and weaknesses, comparing 3D printed Nitinol with traditionally produced nitinol.
Computer based design and method development.
Development of the computer method for (semi-) automatic stent graft design matching patient anatomy (including fenestrations). FEA for optimized stent design, considering factors like blood flow and wall stress.
Production of an anatomically matching stent.
The possibilties of producing an anatomical matiching stent, including curved stents or stent with an varying diamter. The proposed tests should indicate whether such stent graft designs are possible to produce.
Production of a straigth stent with graft and fenestrations.
Designing the production of a film for the stent as graft.
Production of an anatomically matching stent with graft and fenestations.
In addition, a process must be designed that allows for fenestrations to be put in.
Lab tests of the stent graft with fenestrations and a varying diameter or curved design.
The stent graft should be tested in a lab setting to assess its performance and to identify any problems with the design.
Delivery and manipulation of stent graft.
The delivery device might be based upon the already known EVAR products.
First tests on animal tissue to assess its patency and safety.
The lab setting should simulate living tissue (ex vivo) as accurate as possible to be able to predict behaviour in vivo.
Sterilization and packaging of stents.
A sterilization procedure and packaging process should be designed that delivers a sterile and packed product ready for use in an EVAR procedure.
Animal trials.
Optimize production process.
Clinical trials.